UNIVERSITÀ DEGLI STUDI DI NAPOLI “FEDERICO II”

FACOLTÀ DI INGEGNERIA

Dipartimento di Ingegneria Aerospaziale

**Dottorato di Ricerca in Ingegneria Aerospaziale,
Navale e della Qualità**

Indirizzo Gestione della Qualità Totale
XXIV Ciclo di Dottorato

STATISTICS FOR COMPETITIVE ADVANTAGE AND TECHNOLOGICAL INNOVATION: APPLICATIVE SCENARIOS IN MANUFACTURING INDUSTRY AND RESEARCH CENTRES

TUTOR
Prof. Biagio Palumbo

CANDIDATA
Flaviana Tagliaferri

COORDINATORE
Prof. Antonio Moccia

TABLE OF CONTENTS

INTRODUCTION

The main objective of the research study presented in this thesis is to highlight the strategic role that a systematic and sequential approach to experimentation plays in order to get competitive advantage and technological innovation for both manufacturing industry and research centres.

The efficacy of this approach is demonstrated here by three applicative examples where the appropriate use of statistical knowledge, along with technological knowledge, has allowed to optimize some manufacturing processes, to catalyze the innovation process and to promote the technological transfer. Moreover this approach allows to put into action a virtuous cycle of sequential learning

The manufacturing process improvement and the process innovation are some of the strategic activities carried out today in research and development departments of manufacturing industry and in research centres.

An accurate pre-design (i.e. pre-experimental planning phase) is the solid basis on which a statistical approach has to be built. Following the systematic approach to planning for a designed experiment proposed in Coleman and Montgomery (1993) and Ilzarbe at al. (2008), and just successfully applied in Palumbo (2009), a *pre-design guide sheets* (split up into *pre-design master guide* sheets and *supplementary sheets*) to direct the experimentation, were conceived, customized and implemented for each applicative example.

The use of the pre-design guide sheets provides a way to systematize the process by which an experimentation team does the experimental plan. In fact these sheets drive the experimenter to clearly define the objectives and scope of an experiment and to gather information needed to design an experiment.

This kind of approach and the use of the pre-design guide sheets were highly appreciate especially at Technische Universität and Fraunhofer IWU (Chemnitz, Germany) where they never were seen. The pre-design guide sheets implemented in Germany, for two different research activities, are shown here as *attachment I* and *attachment II* (note that some data are omitted for confidentiality).

The framework of this thesis is designed to describe first of all the main guidelines that were acknowledged from literature and the statistical methodologies studied and applied. Then, three applicative examples, performed in three different technology areas, are discussed to show how the statistical tools were put in practice.

The first case study presented has been developed in a national research centre for technology: CIRTIBS. The second and the third ones have been developed in Avio company, leader in the aerospace propulsion sector, particularly in Pomigliano d'Arco (Naples) site, Avio Centre of Excellence for combustors, reheats and combustion systems production.

The real innovations presented in this thesis are to be found not only in the statistical techniques applied (which were unknown in the specific contexts where the research was developed), and in the many technological results obtained, but also in the proposed approach.

The experience gained was used to manage a national research project: "Study and implementation of high brilliance and energy saving laser source for aerospace component micro-drilling machining" (PON/FIT - fund for technological innovation), currently awaiting for funding from the Ministry of Economic Development.

STATISTICS IN EXPERIMENTATION

The manufacturing process improvement and the process innovation are some of the strategic activities carried out today in research and development departments of manufacturing industry and in research centres. Finding the best solution often requires extensive testing; in order to obtain these results as efficiently as possible is fundamental to adopt adequate experimental procedures and effective data analysis.

According to Czitrom (1999), typically, many engineers and scientists perform one-factor-at-a-time (OFAT) experiments, which vary only one factor or variable at a time while keeping others fixed. They will continue to do so until they understand the advantages of different approach over OFAT experiments, and until they learn to recognize OFAT experiments so they can avoid them.

The design of experiments (DoE) is a methodology for systematically applying statistics to the experimentation process; in many cases it is the best way to establish which variables are important in a process and the conditions under which these variables should work to optimize such process. It is the only tool for the experimenters to perform efficient analysis of a process governed by many parameters.

The DoE was introduced in the 1920s by Sir Ronald A. Fisher in the field of agricultural research. Since then much has been published about the theoretical aspect of DoE, such as Wu and Hamada (2000), Montgomery (2005), Box et al. (2005) and today there is sufficient awareness that OFAT experiments are always less useful than statistically designed experiments.

Through some real examples Czitrom (1999) illustrates the advantages of DoE and shows that the experimental results cannot take into account the interactions between factors when only one factor at a time varying while keeping fixed all the other ones. Otherwise in DoE all factors are varied together and it is the only way to discover interactions between variables. For these and many other reasons Montgomery (2005) says that DoE is a critically important tool for the engineer to improving the performance of a manufacturing process. He also says that the application of experimental design techniques early in process development can result in:

- Improved process yields;
- Reduced variability and closer conformance to nominal or target requirements;
- Reduced development time;
- Reduced overall costs.

However, as Ilzarbe et al. (2008) deduce, after a review of 77 articles about practical DoE application, in the field of engineering, the DoE is a methodology that has been applied from many years in industry to improve quality, but it is still not used as it should be.

These statistical techniques are commonly found in statistics and quality literature but, as pointed out by Tanco et al. (2010), it is hardly used in European industry; there is still a significant gap between theoretical development of DoE and its effective application in industry. Why? On one hand Costa et al. (2006) shows that DoE is not an easy technique to be applied due to limitations in technical knowledge of the product and technologies involved. On the other hand Montgomery (1999) refers the inadequate training in basic statistical concepts and methods by the engineers. Therefore, what is needed is the integration of statistical and technological knowledge. In fact it catalyzes the process innovation and, moreover, it allows to put into action a virtuous cycle of sequential learning.

PRE-DESIGN AND GUIDELINES FOR DESIGNING EXPERIMENTS

In order to help the experimenters to plan all activities needed for a good testing, Coleman and Montgomery (1993) suggest a path which consists of the following seven basic steps:

1. Recognition of and statement of the problem;
2. Choice of factors and levels;
3. Selection of the response variable(s);

pre-design

4. Choice of experimental design;
5. Conduction of the experiment;
6. Data analysis;
7. Conclusions and recommendations (followed by monitoring and/or confirmatory test).

Certainly an accurate pre-design is the solid basis on which a statistical approach has to be built.

The pre-design is pre-experimental planning phase, in other words it is all that precedes the definition and execution of experiments, and corresponds to the steps from 1 to 3 suggested.

The first step means to elaborate and write clearly the statement of problem; it is an obvious step but it is harder than it may appear. It is especially needed in a working team so that everyone has a clear idea of the aim.

The selection of the response variable(s) and the choice of the factors, with their levels, is really not a simple issue. It is a crucial task and requires adequate knowledge.

The potential design factors are those parameters that the experimenter considers influence on the process in study; he must choose the range over which these factors will be varied too. About the response variable(s), quoting Montgomery (2005), "*the experimenter should be certain that this variable really provides useful information about the process under study. Most often, the average or standard deviation (or both) of the measured characteristic will be the response variable. Multiple responses are not unusual. Gauge capability (or measurement error) is also an important factor. If gauge capability is inadequate, only relatively large factor effects will be detected by the experiment or perhaps additional replication will be required*".

Therefore, steps 2 and 3 represent the phases where, synthesis of statistical and technological skills, is more required. In fact, to choose a good selection of factors and response variable(s) it is necessary not only to understand the statistical logic, but also to have a good process knowledge.

Who has both statistical and process knowledge, has a competitive tool to perform a good research.

Furthermore, Coleman and Montgomery (1993) present *pre-design guide sheets* (split up into *pre-design master guide* sheets and *supplementary sheets*) to direct the experimentation.

These pre-design sheets force the experimenter to face up to fundamental questions from the early phases of the experimental activity and, moreover, they facilitate and catalyze the interaction between statistical and technological competences.

The master guide sheets contain information about the objective of the experimentation, the relevant background, the response variables and the factors (i.e., control, held-constant and nuisance factors). The supplementary sheets detail the technological relationship between the control factors and the response variables, in terms of the expected main effects and interactions. Moreover, for each quantitative control factor, the normal level and range as well as the measurement precision are specified.

Obviously it is necessary to customize the guide sheets in order to make them more appropriate and comprehensive in the specific technological and organizational context in which they are used.

In each case study following presented, the use and the implementation of pre-design guide sheets allowed the team to carry out the best design of experiment.

Two examples of pre-design guide sheets are shown here as attachment.

THE DESIGN OF EXPERIMENT

According to Hahn (1984) "*The major contribution of the statistical plan was to add discipline to the experiment and to help ensure that it would result in as valid conclusion as possible, subject to the constraints imposed by the testing situation*".

If the pre-design is done correctly, to choose a good DoE is not so hard. To Choose design involves the consideration of sample size (number of replicates), the selection of a suitable run order for the experimental trials, and the determination of whether or not blocking or other randomization restrictions are involved.

Generally, *factorial designs* (with all several special cases of the general factorial design) are very efficient tools when an experiment involves several factors and it is necessary to study the joint effect of the factors on a response.

It is good to remember that the experiments performed with the DoE are iterative. It would be a mistake to schedule a single, large, exhaustive experiment, because this methodology is based on progressive acquisition of knowledge. Two main phases can be identified: *screening* and *optimization*.

Typically, screening or characterization experiments are used to determinate which process parameters affect the response. The next phase is the optimization, which has the scope to determine the region in the important factors that leads to the best possible response.

It is important to point out that basic statistical methods applied, as factorial design and ANalysis Of VAriance (ANOVA), are extensively treated in literature, for example in Montgomery (2005) or Erto (2008), therefore, they have been applied without any explicit introduction or analytical formulation in this work.

MULTI RESPONSE OPTIMIZATION USING THE DESIRABILITY FUNCTION

The problems related to develop a strategy in order to jointly optimize more than one response simultaneously are known as multi-response optimization (MRO) problems. There are several methods proposed in the literature for solving MRO problems (Derringer and Suich 1980; Kros and Mastrangelo 2001; Fogliatto 2008). In *Paper I* a procedure of optimization based on the use of "desirability" was proposed.

In statistics "desirability" functions are functions that transform a set of properties into a single target and contain information about a set of responses Y_i $(i = 1, 2, \dots, 5)$ to optimize simultaneously.

According to Ribardo (2003), many statistician wrote about desirability functions and references include (Del Castillo et al. 1996; Derringer 1994; Derringer and Suich 1980; Harrington 1965, Kim and Lin 2006). Without loss of generality, it is conventional to restrict the range of the desirability functions to the [0, 1] closed interval. Harrington (1965) introduced the first desirability functions. Exponential functional forms were selected to calculate the desirabilities associated with individual criteria, Y_i, and the use of the geometric mean for weighting these criteria together to calculate overall desirability.

Derringer (1994) and Derringer and Suich (1980) criticized the functional forms and weighting scheme in Harrington (1965) for being overly rigid. As an alternative, they suggested a family of functions that permitted the target value to be anywhere in the region between product specifications. In (Del Castillo et al. 1996) an improvement of the individual criteria desirabilities of Derringer is proposed with the aim to reach greater smoothness and differentiability. Afterwards the vulnerability of previous desirability formulations because of sensitivity to dependencies among the Y_i was criticized in (Kim and Lin 2006). Montgomery (2001) concluded with a proposed "maxi/min" strategy for weighting desirabilities associated with individual criteria together to replace the generalized geometric mean of Derringer and Suich (1980). They also proposed modified functions for the individual criteria to account for prediction errors in the response surface models. Recent trends in process design have been strongly influenced by so called "six sigma" methodologies and associated design concepts (Harry1994 and Pande et al. 2000).

Without deepening further it is easy to understand that the notion of desirability has had many developments across the years that contributed to make a multi-response optimization based on the desirability a really consolidated methodology.

In *Paper II* the procedure proposed in Derringer and Suich (1980) is adopted. Entering into details: the first step for the experimenter is to transform each response Y_i $(i = 1,\ 2, \dots, 5)$ into an individual response of desirability d_i $(0 \leq d_i \leq 1\, ; i = 1, 2, \dots, 5)$. This is one of the desirability functions that transform each response variable onto a [0, 1] scale where 1 is the most desirable value and 0 is unacceptable. The desirability function d_i adopted in the proposed case study comes from the one-sided-desirability transformation proposed in Derringer and Suich (1980). The function d_i increases as the response Y_i increases and the target is to maximize the response itself. Results:

$$d_i = \begin{cases} \left(\frac{Y_i - Y_{i,min}}{Y_{i,max} - Y_{i,min}}\right)^r & Y_{i,min} \leq Y_i \leq Y_{i,max} \\ 0 & otherwise \end{cases} \tag{1}$$

where r is a weight that can be assigned to change the shape of the desirability transformation. In order to simultaneously optimize all the responses , the second step is to combine the individual desirability in an overall desirability function Df. Several methods are available in the literature (Kros and Mastrangelo, 2001). In *Paper II* the multiplicative method proposed in Derringer and Suich (1980) was adopted. Results:

$$Df = \left(d_1^{w_1} * d_2^{w_2} * \ldots * d_5^{w_5}\right)^{1/\sum_{i=1}^{5} w_i} \tag{2}$$

where w_i are the response weights.

THE RELATED FACTORS

Generally, in a testing, an appropriate range of values (where the response variables should be evaluated) can be associated for each factor involved. The experimental region results from product of all factor ranges and is regular when is like a cube in *n*-dimensions (where *n* is the number of factors involved).

Sometimes one factor's desirable range depends on the level of another factor, therefore this two factors are related. This relationship between factors, for example, may be due to technological reasons. The experimental region is not regular and it is reflected in the experimental design, so the analysis of related factor design cannot be standard.

To solve this issue Taguchi (1987) introduces the sliding levels strategy. He removes the interaction between two related factors re-coding the levels of both factors and transforms an irregular experimentation region into a regular one.

Nested design

Hamada and Wu (1995) propose an alternative analysis viewing the sliding factor level design as nested design. In fact, as discussed, in certain multifactor experiments the levels of one factors (e.g. factors B) are similar but not identical for different levels of another factor (e.g. A). Montgomery (2005) call such arrangement a *nested*, or hierarchical design, with the levels of factor B nested under the levels of factor A.

The nested design analysis evaluates the significance of the nested factor in relation to the level of the factor to which is related and can be done either in the case where the nested factor is qualitative and quantitative. In the following we neglect the case of qualitative factor, and we consider the case where the factor is quantitative.

Figure 1 shows a design where the factor A is a laser peek power and the factor B is a pulse width of laser beam for a laser machining process. Technological restrictions not allow to set the same value of a pulse width for both peak power level selected. In that case the pulse width is nested under peek power; this is a typical example of nested design.

The 2^2 factorial design would enable the experimenter to investigate the main effects of each factor and to determinate whether the factors interact. Different issue is for the shown example because the levels of factor B is not the same for each level of factor A.

As an example, this plan can be analyzed in nested perspective in the field of laser machining, evaluating the significance of peak power as standard factor and the pulse width as related to the level of peak power.

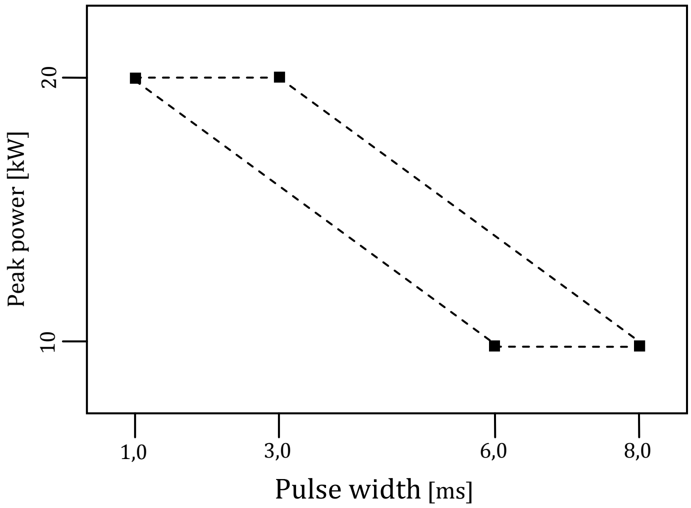

Figure 1 Nested Design

Through this analysis we will be able to evaluate both the significance of the change from 1 to 3 ms at 20 kW and from 6 to 8 ms at 10 kW.

The linear statistical model for the two-stage nested design is:

$$y_{ijk} = \mu + \tau_i + \beta_{j(i)} + \varepsilon_{(ij)k}$$
$$i = 1,2,...,a;$$
$$j = 1,2,...,b;$$
$$k = 1,2,...,n;$$

μ = overall mean
τ_i = effect of A at at ith level
$\beta_{j(i)}$ = effect of B at jth level related to A at ith level
$\varepsilon_{(ij)k}$ = error of kth observation for ith and jth levels of A and B

That is, there are *a* levels of factor A, *b* levels for factor B nested under each level of A, and *n* replicates. The subscript *j(i)* indicates that the *j*th level of factor B is nested under the *i*th level of factor A. It is convenient to think of the replicates as being nested within the combination of level of A and B; thus, the subscript *(ij)k* is used for the error term.

This is a balanced nested design because there are an equal number of levels of B within each level of A and an equal number of replicates. Because every level of factor B does not appear with every level of factor A, there can be no interaction between A and B.

The total corrected sum of square is:

$$\sum_{i=1}^{a}\sum_{j=1}^{b}\sum_{k=1}^{n}\left(y_{ijk}-\bar{y}_{\bullet\bullet\bullet}\right)^2=\sum_{i=1}^{a}\sum_{j=1}^{b}\sum_{k=1}^{n}\left[\left(\bar{y}_{i\bullet\bullet}-\bar{y}_{\bullet\bullet\bullet}\right)+\left(\bar{y}_{ij\bullet}-\bar{y}_{i\bullet\bullet}\right)+\left(y_{ijk}-y_{ij\bullet}\right)\right]^2$$

$$\sum_{i=1}^{a}\sum_{j=1}^{b}\sum_{k=1}^{n}\left(y_{ijk}-\bar{y}_{\bullet\bullet\bullet}\right)^2=bn\sum_{i=1}^{a}\left(\bar{y}_{i\bullet\bullet}-\bar{y}_{\bullet\bullet\bullet}\right)^2+n\sum_{i=1}^{a}\sum_{j=1}^{b}\left(\bar{y}_{ij\bullet}-\bar{y}_{i\bullet\bullet}\right)^2+\sum_{i=1}^{a}\sum_{j=1}^{b}\sum_{k=1}^{n}\left(y_{ijk}-\bar{y}_{ij\bullet}\right)^2 \qquad (3)$$

$$\bar{y}_{\bullet\bullet\bullet}=\frac{\sum_{i=1}^{a}\sum_{j=1}^{b}\sum_{k=1}^{n}y_{ijk}}{abn}$$

$$\bar{y}_{i\bullet\bullet}=\frac{\sum_{j=1}^{b}\sum_{k=1}^{n}y_{ijk}}{bn}\quad i=1,.......,a;$$

$$\bar{y}_{\bullet j\bullet}=\frac{\sum_{i=1}^{a}\sum_{k=1}^{n}y_{ijk}}{an}\quad j=1,.......,b;$$

$$\bar{y}_{ij\bullet}=\frac{\sum_{k=1}^{n}y_{ijk}}{n}\quad i=1,.......,a;\ j=1,.......,b;$$

because the three cross-product terms are zero. The *Equation (3)* indicate that the total sum of squares can be partitioned into a sum of squares due to factor A, a sum of squares due to factor B under level A, and a sum of squares due to error.

Symbolically the *Equation (3)* becomes :

$$SS_T = SS_A + SS_{B(A)} + SS_{(E)} \qquad (4)$$

There are *(abn-1)* degrees of freedom for SS_T, *(a-1)* degrees of freedom for SS_A, *a(b-1)* degrees of freedom for $SS_{B(A)}$, and *ab(n-1)* degrees of freedom for error.

Moreover *(abn-1) = (a-1) +a(b-1) + ab(n-1).*

If the errors are NID(0, σ^2), we may divide each sum of square on the right of *Equation (4)* by its degrees of freedom to obtain independently distributed mean squares such that the ratio of any two mean squares is distributed as Fischer distribution.

The appropriate statistics for testing the effects of factor A and B depend on whether A and B are fixed or random.

If factors A and B are fixed, we assume that:

$$\sum_{i=1}^{a} \tau_i = 0 \quad \text{and} \quad \sum_{j=1}^{b} \beta_{j(i)} = 0 \qquad (\, i = 1,2,\ldots,a).$$

That is, the A treatment effects sum to zero, and the B treatment effects sum to zero within each level of A. The *Table 1* indicates that if the levels of A and B are fixed, the hypothesis H_0:τ_i = 0 is tested by MS_A/MS_E and the hypothesis H_0:$\beta_{j(i)}$= 0 is tested by $MS_{B(A)}/MS_E$.

E(MS)	A (Fixed) B (Fixed)
$E(MS_A)$	$\sigma^2 + \frac{bn\sum\tau^2}{a-1}$
$E(MS_{B(A)})$	$\sigma^2 + \frac{n\sum\sum\beta^2_{j(i)}}{a(b-1)}$
$E(MS_E)$	σ^2

Table 1 Expected mean squares in the Two-Stage Nested Design

The test procedure for a two-stage nested design is summarized in an analysis of variance table as show in *Table 2*

Source of Variation	Sum of Squares	Degrees of Freedom	Mean Square
A	$bn\sum\left(\bar{y}_{i\bullet\bullet}-\bar{y}_{\bullet\bullet\bullet}\right)^2$	$a-1$	MS_A
B within A	$n\sum\sum\left(\bar{y}_{ij\bullet}-\bar{y}_{i\bullet\bullet}\right)^2$	$a(b-1)$	$MS_{B(A)}$
Error	$\sum\sum\sum\left(y_{ijk}-\bar{y}_{ij\bullet}\right)^2$	$ab(n-1)$	MS_E
Total	$\sum\sum\sum\left(y_{ijk}-\bar{y}_{\bullet\bullet\bullet}\right)^2$	$abn-1$	

Table 2 Analysis of Variance Table for the Two-Stage Nested Design

The formulas for the sums of squares are:

$$SS_A = \frac{1}{bn}\sum_{i=1}^{a} y_{i\bullet\bullet}^2 - \frac{y_{\bullet\bullet\bullet}^2}{abn}$$

$$SS_{B(A)} = \frac{1}{n}\sum_{i=1}^{a}\sum_{j=1}^{b} y_{ij\bullet}^2 - \frac{1}{bn}\sum_{i=1}^{a} y_{i\bullet\bullet}^2$$

$$SS_E = \sum_{i=1}^{a}\sum_{j=1}^{b}\sum_{k=1}^{n} y_{ijk}^2 - \frac{1}{n}\sum_{i=1}^{a}\sum_{j=1}^{b} y_{ij\bullet}^2$$

$$SS_T = \sum_{i=1}^{a}\sum_{j=1}^{b}\sum_{k=1}^{n} y_{ijk}^2 - \frac{y_{\bullet\bullet\bullet}^2}{abn}$$

Moreover the sum of error can be written as:

$$SS_{B(A)} = \sum_{i=1}^{a}\left[\frac{1}{n}\sum_{j=1}^{b} y_{ij\bullet}^2 - \frac{y_{i\bullet\bullet}^2}{abn}\right].$$

This expresses the idea that $SS_{B(A)}$ is the sum of squares between levels of B for each level of A, summed over all the levels of A.

For a two-stage nested design the residuals are:

$$e_{ijk} = y_{ijk} - \hat{y}_{ijk}$$
$$\hat{y}_{ijk} = \hat{\mu} + \hat{\tau}_i + \hat{\beta}_{j(i)}$$

In the hypothesis that:

$$\sum_{i=1}^{a} \tau_i = 0 \quad \text{and} \quad \sum_{j=1}^{b} \beta_{j(i)} = 0 \qquad (\text{ i} = 1,2,\ldots,\text{a})$$

are:

$$\hat{\mu} = \overline{y}_{\bullet\bullet\bullet}, \qquad \hat{\tau}_i = \overline{y}_{i\bullet\bullet} - \overline{y}_{\bullet\bullet\bullet}, \qquad \text{and} \qquad \hat{\beta}_{j(i)} = \overline{y}_{ij\bullet} - \overline{y}_{i\bullet\bullet};$$

the estimated values are:

$$\hat{y}_{ijk} = \overline{y}_{\bullet\bullet\bullet} + (\overline{y}_{i\bullet\bullet} - \overline{y}_{\bullet\bullet\bullet}) + (\overline{y}_{ij\bullet} - \overline{y}_{i\bullet\bullet}) = \overline{y}_{ij\bullet}$$

and the residuals for a two-stage design are:

$$e_{ijk} = y_{ijk} - \overline{y}_{ij\bullet}$$

The residual analysis graphs are useful to interpret the results of a nested design where B(A) is significant. In fact, the variability of B for each level of A can evaluated plotting the residual values versus A levels.

There are cases in which some factors are arranged in a factorial plan and other factors are nested; this kind of design is called *nested factorial design.*

By way of example, a model of experimental design with three factors of which two related, is:

$$y_{ijkl} = \mu + \tau_i + \beta_{j(i)} + \varepsilon_{(ijk)l} + \gamma_k + (\tau\gamma)_{ik} + (\tau\beta)_{kj(i)}$$

$$\begin{aligned} i &= 1,2,..., a; \\ j &= 1,2,..., b; \\ k &= 1,2,..., c; \\ l &= 1,2,..., n; \end{aligned}$$

τ_i = effect of A at *i*th level
$\beta_{j(i)}$ = effect of B at *j*th level related to A at *i*th level
$\varepsilon_{(ijk)l}$ = error of *l*th observation for the *i*th, jth and *k*th levels of A, B and C
γ_k = effect of C at *k*th level
$(\tau\gamma)_{ik}$ = interaction between A and C
$(\tau\beta)_{kj(i)}$ = interaction between B and C at *i*th level of A

The analysis of variance for this kind of design combines the statistics techniques for nested design and for factorial design.

The nested design analysis models the effect of the nested factor separately at each level of its associated factor.

Hamada and Wu (1995) proposed a nested-effects modelling (NEM) approach by using a regression model with nested effects. Consider the case of two related factors where factor B is nested under A. If the factor A is qualitative, they proposed analyzing the effect of B at each level of A. If B is quantitative with more than two levels, the linear and quadratic effects of B at the *i*th level of A, denoted by $B_l|A_i$ and $B_q|A_i$, should be analyzed.

According to this approach there is no regressor associated with the interaction of A and B, but this is taken into account by creating a regressor for each level of A, which takes into account the effect of B. In addition there are one or more conditional regressors on whether the factor B has two or more levels.

The Table 3 shows particular coding of regressors for a nested factorial design consists of two related factors, A and B, both at three levels.

This approach takes into account the potential interaction between related factors.

A	B	$A_{1,2}$	$A_{1,3}$	A_l	A_q	$B_l \vert A_1$	$B_q \vert A_1$	$B_l \vert A_2$	$B_q \vert A_2$	$B_l \vert A_3$	$B_q \vert A_3$
1	1	-1	-1	-1	1	-1	1	0	0	0	0
1	2	-1	-1	-1	1	0	-2	0	0	0	0
1	3	-1	-1	-1	1	1	1	0	0	0	0
2	1	1	0	0	-2	0	0	-1	1	0	0
2	2	1	0	0	-2	0	0	0	-2	0	0
2	3	1	0	0	-2	0	0	1	1	0	0
3	1	0	1	1	1	0	0	0	0	-1	1
3	2	0	1	1	1	0	0	0	0	0	-2
3	3	0	1	1	1	0	0	0	0	1	1

Table 3 Coding of regressors for a nested factorial design

If A is qualitative with three levels, two regressors, denoted $A_{1,2}$ e $A_{1,3}$, can made, where $A_{i,j}$ represents the contrast between levels *i* and *j* of A.
If A is quantitative, the linear and quadratic effects of A, A_l e A_q, should be substituted for $A_{1,2}$ e $A_{1,3}$.

Hybrid strategy for sliding factors based on response surface modelling

Cheng et al. (2006) observe that, if A is a quantitative factor, we may need to predict the response *y* at a setting value of A, say x_A^*, not included in the experimental plan. To obtain this, a fitted model of B at A = x_A^* is needed. However, such a model is not available in the NEM approach because an NEM offers fitted models of B only for each levels of A. Consequently, the prediction of response y, at value of A not included in the experimental plan, cannot be achieved in a NEM approach. Therefore they propose an analysis method based on the response surface methodology (RSM).
The RSM is extensively treated in literature, for example in Myers and Montgomery (1995), therefore, no other details are given about it.
Generally, in a factorial design, the experimental region, say R_E, has a regular shape. Contrariwise for an experiment with sliding factors, the experimental region is irregular.

In these cases the RSM can be applied but it is necessary to find a cuboidal region that covers exactly the experimental region. To achieve it a special coding for each factor levels is needed.

The lowest level of each factor has to be coded as −1 and the highest level as +1. Other settings of the factor is then proportionally coded according to their distances from the lowest one.

In this coding, the cuboidal region $[-1, +1]^k$ is the smallest cube to cover the R_E. Cheng et al. (2006) call this region as *modeling region* and denote it by R_M.

The RSM can then be applied in the modelling region to develop an empirical model. Unlike factorial designs with regular experimental region, the design points in a sliding-level experiment do not spread uniformly on the whole modelling region.

The *Figure 2* shows an example with two factors. In red is the experimental region R_E, in black the modelling region R_M.

Because there are no design points located in $R_M \backslash R_E$, we have no information about the response surface over $R_M \backslash R_E$. The fitted model may fit well only in R_E, but not in the whole R_M.

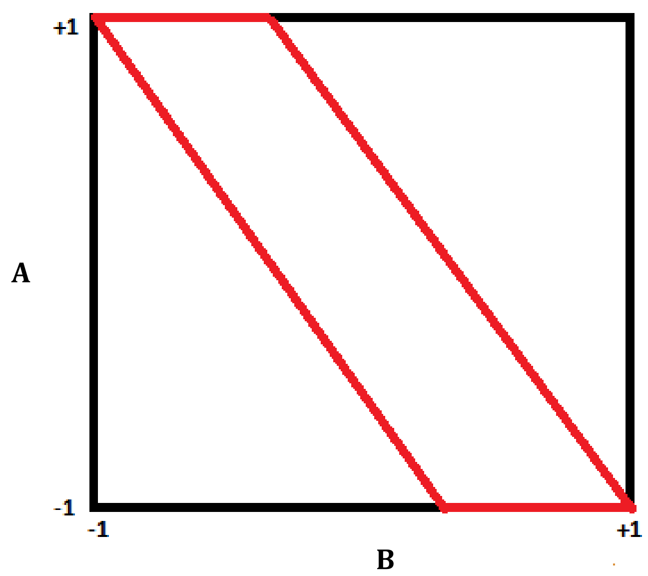

Figure 2 The experimental region R_E in red and the modeling region R_M in black

When a fitted model is obtained, prediction can be easily done in the RSM approach. Its prediction is an interpolation in R_E but an extrapolation in $R_M \backslash R_E$.
Cheng et al. (2006) suggest to adopt the *hybrid strategy* that combines NEM and RSM as follows:

1. Start from a NEM (which enables to identify the significant effects)

2. Translate the fitted NEM into an RSM model through equations that relate the parameters in the two models.

The resulting RSM model can then be used for response prediction.
To clarify briefly consider a experimental plan with three factors A, B(A) and C at two levels; we can write:

$$\hat{y}(B, C|A = -1) = \hat{\beta}_0^{-1} + \hat{\beta}_1^{-1} B(A = -1) + \hat{\beta}_2^{-1} C + \hat{\beta}_3^{-1} BC(A = -1)$$

$$\hat{y}(B, C|A = 1) = \hat{\beta}_0^{1} + \hat{\beta}_1^{1} B(A = 1) + \hat{\beta}_2^{1} C + \hat{\beta}_3^{1} BC(A = 1)$$

where $\hat{\beta}_0^{-1}$, $\hat{\beta}_1^{-1}$, $\hat{\beta}_2^{-1}$, $\hat{\beta}_3^{-1}$, $\hat{\beta}_0^{1}$, $\hat{\beta}_1^{1}$, $\hat{\beta}_2^{1}$, $\hat{\beta}_3^{1}$ are the parameters whose values are to be estimated by least squares method, but is necessary to adapt some of them at the RSM model. This step is needed for the parameters which are different for NEM and RSM.
If for A=1 with B(A) from -1 to 1, in NEM approach the response variable increases of δ quantity, in RSM coding, when A=1 than B(A) changes between -1 and 1: for example from -1 and -0.2. (See *Figure 1*)
However, the variation δ of the response variable must still be the same even for the RSM model.
Then, to obtain the value of parameter related to B(A), in RSM prospective:

$$[1 - (-1)]\hat{\beta}_1^i = [-0.2 - (-1)]b_1^i$$

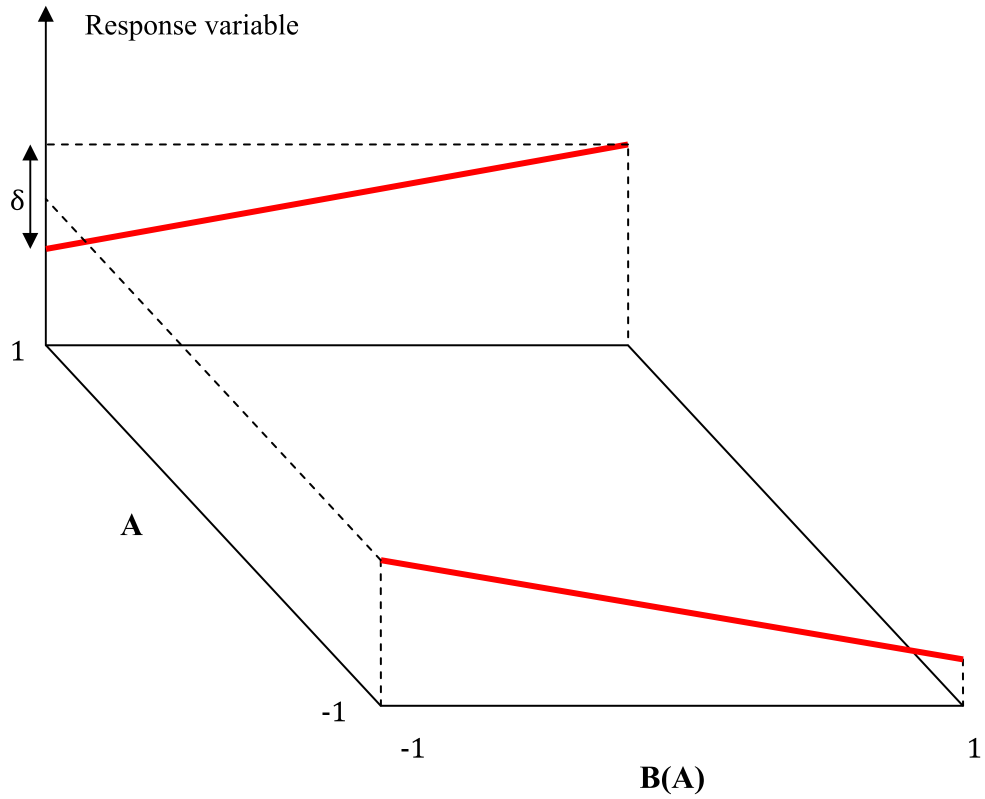

Figure 3 Response variable from NEM point of view

therefore, when $\hat{\beta}_1^i$ is known (in NEM prospective), b_1^i.can be evaluated too.

Moreover from the NEM point of view, the product B*C can be equal to -1 or 1 (because both B and C are coding as -1 or 1); from the RSM point of view the product B*C can be also different from -1 or 1 (in the previous example, the product B*C can be equal to -1, 1, -0.2, 0.2).

To estimate b_3^i by least squares is necessary to consider only BC expressed by RSM coding. So the estimation is composed of a constant (the same constant of estimated model in NEM prospective) and of product between BC and the estimate of relevant parameter b_3^i.

Putting $b_0^i = \hat{\beta}_0^i, b_2^i = \hat{\beta}_2^i$ and using b_1^i e b_3^i is possible to write the RSM model, defined for A = -1 e A = 1.

$\hat{y}\ (x_B, x_C | x_A = i) = b_0^i + b_1^i x_B + b_2^i x_C + b_3^i x_B x_C$ where i = -1, 1

At this point x_A must be put into the RSM, so:

$$\hat{y}\,(x_A, x_B,\, x_C) = \lambda_0 + \lambda_1 x_A + \lambda_2 x_B + \lambda_3 x_C + \lambda_{12} x_A x_B + \lambda_{13} x_A x_C + \lambda_{23} x_B x_C + \lambda_{123} x_A x_B x_C \quad (5)$$

Two models, which depend only from x_B and x_C can be obtain fixing first $x_A = 1$ and than $x_A = -1$. Therefore, writing:

$$\begin{cases} \lambda_0 + \lambda_1 = b_0^1 \\ \lambda_0 - \lambda_1 = b_0^{-1} \\ \lambda_2 + \lambda_{12} = b_1^1 \\ \lambda_2 - \lambda_{12} = b_1^{-1} \\ \lambda_3 + \lambda_{13} = b_2^1 \\ \lambda_3 - \lambda_{13} = b_2^{-1} \\ \lambda_{23} + \lambda_{123} = b_3^1 \\ \lambda_{23} - \lambda_{123} = b_3^{-1} \end{cases}$$

we can solve the *Equation (5)*.

STATISTICAL CHARACTERIZATION OF FIBER LASER MACHINING OF TITANIUM ALLOY

The applicative example, presented in *Paper I*, concerns a preliminary statistical study on laser machining of titanium alloy. This activity has been developed in CIRTIBS research centre.

The aim of this research activity was to characterize the laser engraving process; that was, to detect which process parameters affect the depth of machined volume and the quality of the machined surface in terms of roughness. Consequently this activity involves both statistical and technological aspects.

The results obtained have immediately showed the strategic role that a systematic approach to planning for a designed experiment can play in technological process innovation in fact novel technological information were already obtained in a screening experimental phase conducted with a statistical approach and described in the *Paper I*.

TECHNOLOGICAL CONTEXT

Laser machining is one of the most adopted technologies in rapid prototyping to produce tool and mould operations. As stated by Chryssolouris (1991), Meijer (2004) and Dubey and Yadava (2008), a laser beam is used to ablate a solid bulk, following predetermined patterns. The sculpture is obtained by repeating this process on each successive thin layer. However, the degree of shape precision, the Material Removal Rate (MRR) and the surface quality during the engraving process strictly depend on several factors like material properties, laser source characteristics and the process parameters.

The Laser machining tests were carried out on Ti6Al4V alloy sheet, 4 mm thick, using a Q-Switched 30 W Yb:YAG fiber laser (Lasit Fly Fiber 30W), with fundamental wavelength $\lambda = 1064$ nm, duration time of 50 ns and pulse frequency variable in the range of 30÷80 kHz, pulse energy up to 1 mJ.

The laser beam is first moved through two galvanometer mirrors, and then it is focused by a "flat field" lens, with a focal length of 160 mm, onto the workpiece. The final focused beam diameter is about 100 μm. The laser system is controlled through a PC, which allows the generation of the geometric patterns and the setting of the following process parameters: the mean beam power (Pm), the pulse frequency and the scan speed.

In order to perform the engraving tests four Ti6Al4V alloy plates, 60x60x4 mm^3 in size, were used. A square areas 5x5 mm^2 in plane dimension were machined at nominal maximum mean beam power (30 W).

METHODOLOGICAL APPROACH

The statistical methodologies applied in this first screening experimental phase are two-level fractional factorial design and Analysis of Variance. Following the systematic approach to planning designed two pre-design guide sheets were drew up and implemented. The control factors adopted were five, four of them were quantitative, the last one was qualitative. In this screening experimental phase a 2^{5-1} design was adopted. This design, with I = ABCDE (defining relation), is a resolution V design, so no main effect or two-factor interaction is aliased with other main effects.

Regarding main results, the influence of the process parameters on the depth of machined volume and the roughness of the engraved surface has been evaluated.
In addiction a predictive model of the machined volume was proposed and verified. In practice experimental results have shown that, for each adopted pulse frequency, machined volume linearly depend on the total amount of released energy.
At last the process map in terms of Material Removal Rate (MRR) and roughness has been evaluated and discussed too.
Moreover, since the results obtained in this screening phase arise from a sound systematic approach, they enabled to plan a following experimental phase on optimization and robustness. *Paper I* does not deal with the subsequent experimental phases because most of them are still in progress.

PAPER I

Statistical analysis of fiber laser machining of titanium alloy

F. Tagliaferri[a], N. Pagano[b], C. Leone[b], B. Palumbo[a]

[b]*Department of Aerospace Engineering, University of Naples "Federico II", Naples, Italy*
[a]*Department of Materials and Production Engineering, University of Naples "Federico II", Naples, Italy*

Abstract

In this work a preliminary statistical study on laser machining of titanium alloy is presented. Laser machining tests were carried out on Ti6Al4V alloy sheet, 4 mm thick, using a Q-Switched 30 W Yb:YAG fiber laser. The aim of the paper is to characterize the laser engraving process; that is, to detect which process parameters affect the depth of machined volume and the quality of the machined surface in terms of roughness. The examined parameters were: the lease beam scan speed, the pulse frequency, the distance between the linear patterns of two consecutive laser scans (step), the number of repetitions of the geometric pattern and the scanning strategy. A two-level fractional factorial design and ANalysis Of VAriance (ANOVA) were applied. In addition experimental results have shown that, for each adopted pulse frequency, the machined volume linearly depend on the total amount of released energy. Besides the process map in term of Material Removal Rate (MRR) and roughness has been evaluated and discussed too.

Keywords: Laser machining, fiber laser, Design of Experiment (DOE), ANOVA

1. Introduction

Laser machining is one of the most adopted technologies in rapid prototyping to produce tool and mould operations. A laser beam is used to ablate a solid bulk, following predetermined patterns [1-3]. The sculpture is obtained by repeating this process on each successive thin layer. Compared to traditional machining, this method has some advantages, such as: greater flexibility of use, no mechanical contact with the surface, a reduction in industrial effluents (i.e. no acid, solvent or dielectric oils are required) and a fine accuracy of machining, even with complex forms in injection moulding [4-5]. However, the degree of shape precision, the Material Removal Rate (MRR) and the surface quality during the engraving process strictly depend on the material properties, the laser source characteristics and the process parameters. In order to obtain low roughness and high MRR a process of optimization is required [6-10].

In this paper laser engraving of Ti6Al4V alloy has been studied by using a Q-Switched 30 W Yb:YAG fiber laser. In particular the influence of the process parameters on the depth of machined volume and the roughness of the engraved surface has been evaluated.

This paper involves both statistical and technological aspects. The statistical methodologies applied in this first screening experimental phase, two-level fractional factorial design and ANalysis Of VAriance (ANOVA), are extensively treated in the literature (for example in [11]), and so they will be applied without any explicit introduction or analytical formulation.

In addiction a predictive model of the machined volume was proposed and verified. In practice experimental results have shown that, for each adopted pulse frequency, machined volume linearly depend on the total amount of released energy.

At last the process map in terms of Material Removal Rate (MRR) and roughness has been evaluated and discussed too.

2. Equipment, material and experimental design

2.1. Laser equipment

The engraving tests were performed by using a Q-Switched 30 W Yb:YAG fiber laser (Lasit Fly Fiber 30W), with fundamental wavelength λ = 1064 nm, duration time of 50 ns and pulse frequency variable in the range of 30÷80 kHz, pulse energy up to 1 mJ.

The laser beam is first moved through two galvanometer mirrors, and then it is focused by a "flat field" lens, with a focal length of 160 mm, onto the workpiece. The final focused beam diameter is about 100 µm. The laser system is controlled through a PC, which allows the generation of the geometric patterns and the setting of the following process parameters: the mean beam power (Pm), the pulse frequency and the scan speed.

In Figure 1 the characteristic response of the laser source, in terms of pulse energy and pulse power, is reported as a function of pulse frequency, at different mean power values.

Pulse energy and pulse power play an important role in the laser machining process, by determining the laser beam-material interaction mode and then the amount of machined volume. Their influence will be take into account in this experimental study by changing the pulse frequency.

The adopted experimental conditions, in terms of mean beam power and pulse frequency, are highlighted by circles in Figure 1.

2.2. Material and measurement equipment

The adopted materials is a Alpha/Beta Titanium Alloy (Ti6Al4V), largely applied in medical and aerospace fields. In Table 1 the main thermo-mechanical properties and the chemical composition are reported.

In order to perform the engraving tests four Ti6Al4V alloy plates, 60x60x4 mm^3 in size, were used. A square areas 5x5 mm^2 in plane dimension were machined at nominal maximum mean beam power (30 W).

The depth and the roughness of the engraved cavities were measured by 3D Surface Profilometer Talysurf CLI 2000 by Taylor Hobson. No less than 5 profiles were acquired in the same direction of the scanning speed.

For the analysis of the acquired profiles, a surface analysis software (Taly Map Universal) was adopted, in order to measure the depth of the engraving and the roughness of the engraved surfaces.

In Figure 2 an image of a machined plate, during the measuring process, is reported.

As roughness parameter was used the arithmetic mean of the profile data points, Ra (ISO 1302:2002).

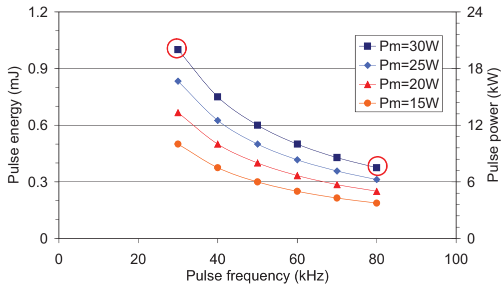

Fig. 1: Pulse energy and pulse power as a function of the pulse frequency at different mean power values (Pm).

Table 1
Main properties and chemical composition of Ti6Al4V alloy.

Properties			Componet (%)	
Density (kg/m^3)		4430	Al	6
Hardness, Brinell		334	Fe	Max 0.25
Ult. Tensile Strength (MPa)		950	O	Max 0.2
Yield Strength, (MPa)		880	Ti	90
Elongation at Break (%)		12	V	4
Young's Modulus (GPa)			113.8	
CTE, 20°C (µm/m °C)			8.6	
CTE, 500°C (µm/m °C)			9.7	
Specific Heat Capacity (J/g °C)			0.5263	
Thermal Conductivity (W/m K)			6.7	
Melting Point (°C)	Solidus		1604	
	Liquidus		1660	
Beta Transition (°C)			980	

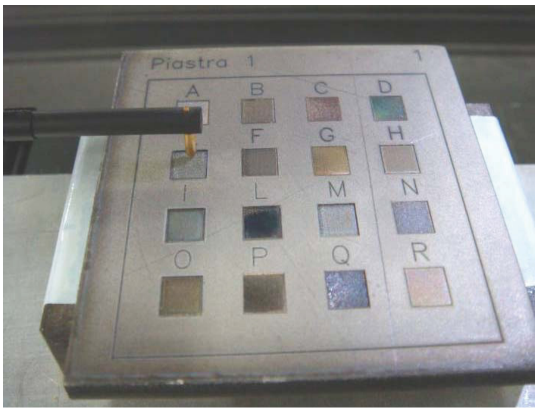

Fig. 2. Example of an engraved sample.

The machined volume was evaluated as product between the mean depth and the plane dimension of the groove [10]. The MRR was quantified as the ratio between the machined volume and the calculated process time.

2.2. Pre-experimental planning, experimental design and set-up

Following the systematic approach to planning designed experiments proposed in [12] and successfully applied in [13], two pre-design sheets (i.e. the main and secondary sheets) were drew up and implemented. These two kinds of sheets catalyze the interaction between statistical and technological competences.

The main sheets contain information about the objective of the experimentation, the relevant background, the response variables and the factors (i.e. control, held-constant and nuisance factors).

On the secondary sheets, for each quantitative control factor, the normal level and range as well as the measurement precision were specified. Moreover the secondary sheets detail the technological relationship between the control factors and the response variables, in terms of the expected main effects and interactions.

In this first experimental phase, the objective was to characterize the laser engraving process; that is, to detect which factors affect the quality of the machining surface in term of depth of machined volume and surface roughness.

For each variable, the normal operating level, the range, the measurement precision and the relationship to the objective were specified on the main sheets. The first step involved listing all factors that came out during team discussions. The second step consisted in classifying each factor as a control, held-constant or nuisance factor [12].

Obviously, different classifications are possible, each strictly related to the specific aims of the experiment.

The following control factors were adopted: scan speed (A), pulse frequency (B), step (C) (distance between two consecutive scan lines), repetition number of the geometric pattern (D) and scanning strategy (E).

The number of repetitions (D) represents the number of the laser beam scanning on the same area. The adopted scanning strategy (E) were two: the first one is based on horizontal lines (//), the other one is based on a sequence of four lines placed at 0°,90° and ±45° (/\).

Factors A, B, C and D are quantitative parameters. Factor E is a qualitative factor that refers to the specific scanning strategy adopted. Figure 3 shows both different scanning strategies.

In this screening experimental phase a 2^{5-1} design was adopted. This design, with I = ABCDE (defining relation), is a resolution V design, so no main effect or two-factor interaction is aliased with other main effects or two-factor interactions, but each main effect is aliased with a four-factor interaction, and each two-factor interaction is aliased with a three-factor interaction.

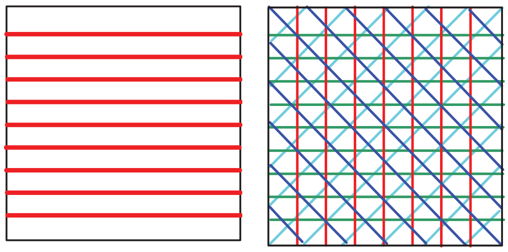

Fig. 3. Scanning strategies.

Table 2
Control factors and their settings.

Control factors	Labels	Low (−)	High (+)	Unit
Scan speed	A	400	1600	mm/s
Frequency	B	30	80	Hz
Step	C	30	60	µm
Repetitions	D	80	120	--
Strategy	E	//	/\	--

Table 3
Matrix for the 2^{5-1} design.

Treatment	A	B	C	D	E=ABCD
a	+	+	-	+	-
b	+	-	+	+	-
c	+	+	+	-	-
d	-	+	+	-	+
e	-	-	+	-	-
f	+	-	-	-	-
g	+	+	+	+	+
h	+	-	-	+	+
i	-	-	-	-	+
l	-	+	-	+	+
m	-	-	-	+	-
n	-	+	+	+	-
o	-	-	+	+	+
p	+	+	-	-	+
q	-	+	-	-	-
r	+	-	+	-	+

Since three-factor (and higher) interactions are negligible, the experimental 2^{5-1} design enables reliable information to be obtained about main effects and two-factor interactions. Table 2 summarizes the levels of control factors and their settings.

Table 3 shows the 2^{5-1} design matrix. For each treatment, 4 replications were executed, giving a total of 64 experimental runs. This number of replications was adopted to provide more consistent response repeatability during this first experimental study.

3. Statistical results and technological considerations

3.1. Statistical analysis of results

The ANOVA method was applied in order to test the statistical significance of the main effects and the two-factor interactions for depth of machined volume and surface roughness. Diagnostic checking was successfully performed via graphical analysis of residuals.

The experimental results for depth of machined volume and surface roughness are shown in Figure 4 using Pareto charts of standardized effects ($\alpha = 0.05$).

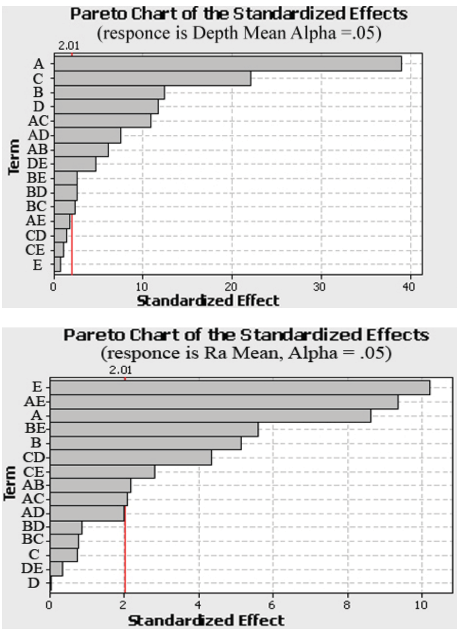

a)

b)

Fig. 4. Pareto charts of standardized effects ($\alpha = 0.05$): **a)** depth of machined volume material; **b)** surface roughness.

Figures 5 and 6 show the main effects and the interaction effects plots for depth (measured in µm) of machined volume, respectively. The significant effects (α =0.05) are highlighted (red boxes). They are the scan speed (A), the pulse frequencies (B), the steep (C) and the repetition (D).

In terms of mean effects the results are not unexpected since the laser beam-material interaction mode depend on the factors A and B, while the working time depend on the factors A, C and D, as also reported in [5, 7 and 10].

Although strategy (E) is not significant, the interaction between the repetition and the strategy (DE) is significant. This result was not expected and requires further technological investigations.

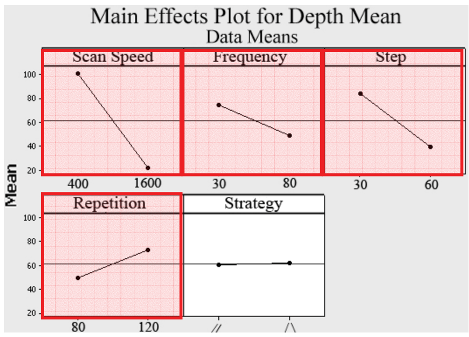

Fig. 5. Main effects plot for depth (in µm) of machined volume.

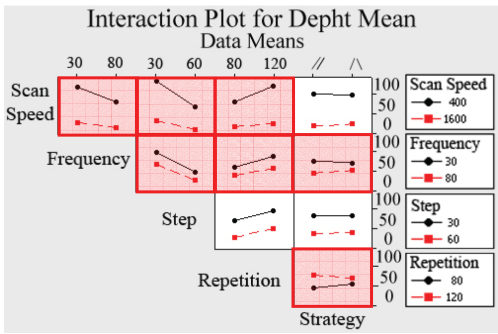

Fig. 6. Interaction effects plot for depth (in µm) of machined volume.

Figures 7 and 8 show the main effects and the interaction effects plots for surface roughness (measured in µm) respectively. The significant effects (α =0.05) are highlighted (red boxes). In terms of main effects of scan speed (A), frequency (B), repetition (D) and strategy (E) the results are in agreement to those observed in [10]. On the contrary the result for step (C) is surprising because, in previously works, its influence was observed [6, 7, 8 and 10].

This contradiction could be first explained taking into account the anti-synergic type interaction between step and repetition (CD) (see Figure 8). It means that the effect of the different level of the repetitions (D) tends to balance the effect of the step (C) [11]. This first interpretation needs further technological investigations.

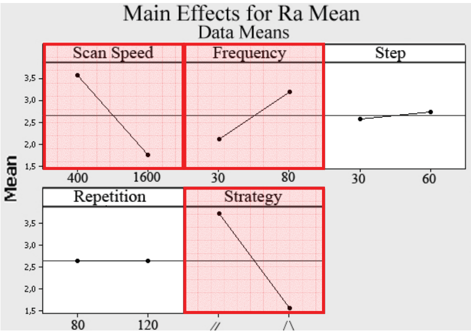

Fig. 7. Main effects plot for surface roughness (μm).

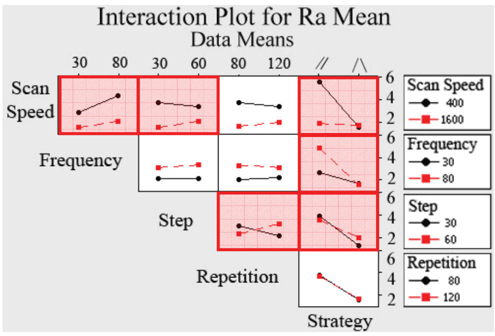

Fig. 8. Interaction effects plot for surface roughness (μm).

3.2. Technological considerations in term of machined volume, roughness and MRR

Since the depth of machined volume strictly depends on the laser beam-material interaction mode and the working time, in order to formulate a predictive model for the machined volume it is possible to use an easy model based on energy consideration, often used for laser machining [7, 14].

The model starts from the equation:

$$V = \alpha \frac{Et}{Q_v} \tag{1}$$

where V is the ablated volume; Et is the total amount of released energy, α is the coefficient of absorption of the materials at the emission wavelength and Q_v is the material vaporization energy for unit volume.

Obviously the model neglects all the energy losses. So, in order to verify the validity of the proposed model, the machined volume was plotted as a function of the total amount of released energy (calculated as product between the mean beam power and the interaction time), as showed in Figure 9.

From Figure 9, it is possible to observe that, as expected, for each adopted pulse frequency (30 and 80 kHz) the machined volume linearly depend on the total amount of released energy.

Furthermore, the different slope of the lines indicates that a different laser beam-material interaction mode occurs changing the pulse frequency as also observed from the ANOVA in terms of depth of machined volume.

In order to obtain indication about both machined volume and surface roughness, the roughness parameter Ra was reported in Figure 10 as a function of the MRR for each treatment shown in Table 3.

In Figure 10 are visible six different groups of treatments, each one indicated by a different symbol (+, ×, ◊, □, ▲, ●), where each treatment is labelled by a letter (see Table 3).

Since high productivity and low roughness are the first requirements, the best process treatments correspond to the ones indicated by the closed dots (b, i and o, also highlighted in Table 3).

On the contrary, the worst working condition corresponds to the process treatments indicated by the squared dots (q and n treatments).

In Figure 10 the images of the obtained surface for the best and the worst cases are reported.

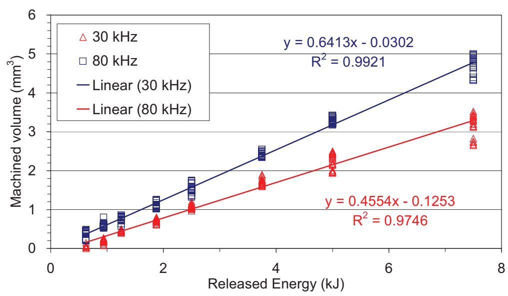

Fig. 9. Machined volume as a function of the total amount of energy. The continuous lines represent the best fitting lines for the two used pulse energy value.

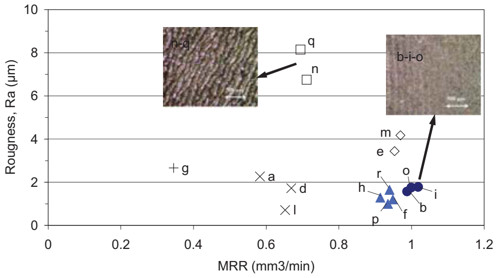

Fig. 10. Roughness, Ra, as a function of the MRR for the different process treatments.

5. Conclusions

This first experimental study concerning the laser engraving of the Ti6Al4V alloy by means of a Q-Switched 30W Yb:YAG fiber laser has sown the strategic role that a systematic approach to planning for a design of experiments plays in technological process innovation.

The results obtained in this first screening experimental phase enabled the factors that affect the depth of the machined volume and the quality of the machined surface in terms of roughness.

In addition, experimental results have shown that, for each adopted pulse frequency, the machined volume linearly depend on the total amount of released energy. At last the best treatments in terms of roughness Ra and MRR have been evaluated too.

Acknowledgements

The authors are particularly grateful to the CIRTIBS Research Centre, for providing the equipments and financial support to develop the present research work.

References

[1] Chryssolouris G., Laser Machining - Theory and Practice. Mechanical Engineering Series, Springer-Verlag, New York Inc., NewYork, 1991.

[2] Meijer J., Laser beam machining (LBM), state of the art and new opportunities. J. of Materials Processing Technology, 149, 2004, pp. 2–17.

[3] Dubey K., Yadava V.. Laser beam machining - A review. I. J. of Machine Tools & Manufacture, 2008, 48, pp. 609–628.

[4] Kaldos, H.J. Pieper, E. Wolf, M. Krause. Laser machining in die making—a modern rapid tooling process. J. of Materials Processing Technology, 155–156, 2004, pp. 1815–1820.

[5] Leone C., Quadrini F., Santo L., Tagliaferri V., Trovalusci F. Nd-YAG laser sculpture of WC punches for micro-sheet forming. Key Engineering Materials, 344, 2007, pp. 783-789.

[6] Leone C., Morace R. E., De Iorio I.. AISI 304 Stainless Steel Engraving by Q-Switched Nd:YAG Nanosecond Laser. J. of the Chinese Society of Mech. Eng., 28 No.2: 217-224, 2007.

[7] Leone C., Lopresto V. and De Iorio I..Wood engraving by Q-switched diode pumped frequency doubled Nd:YAG green laser. Optics and Lasers in Engineering, 47/1: 161-168, 2009.

[8] Lorenz A., Emmelmann C.. Methodical investigations for increasing process capability of short pulse laser ablation in high precision die and mould industry, High-Power Laser Ablation VI. In: Proc. of SPIE, Vol. 6261, pp. 626122-13, 2006.

[9] Cicală E., Soveja A., Sallamand P., Grevey D., Jouvard J.M., The application of the random balance method in laser machining of metals. J. of Mat. Proc Technology , 196:393–401, 2008.

[10] Genna S., Leone C., Lopresto V., Santo L., Trovalusci F., Study of fiber laser machining of C45 steel: influence of process parameters on material removal rate and roughness, Int. J. of Material Forming, 3/1, 2010, pp. 1115-1118.

[11] Montgomery D.C., Design and Analysis of Experiments. Wiley, New York, 2001.

[12] Coleman D.E., Montgomery D.C.: A systematic approach to planning for a designed industrial experiment. Technometrics. 35(1), 1993, pp. 1–12

[13] Palumbo B., De Chiara G., and Marrone R., “Technological Process Innovation via Engineering and Statistical Knowledge Integration” edit by Pasquale Erto, Statistics for Innovation, Springer, 2009.

[14] Duley W.W., CO2 Laser: Effect and applications, Academy Press, New York (1977).

STATISTICAL CHARACTERIZATION AND OPTIMIZATION OF TACK WELDING PROCESS

Avio Group, leader in the aerospace propulsion sector, through its sites, subsidiaries and companies participated in, is a worldwide player. The following case study (extensively described in *Paper II*) has been developed in the Pomigliano d'Arco (Naples) site, Avio Centre of Excellence for combustors, reheats and combustion systems production. Furthermore, is there also an Avio Service, a centre of excellence for overhaul, maintenance and service for aeronautical engines.

TECHNOLOGICAL CONTEXT

Tack-welding is a very common process in aero-engine manufacturing companies. This process uses a power supply to keep an electric arc between electrodes and base materials to melt metals. The contacting metal surfaces of workpieces are held together under pressure exerted by two-shaped copper alloy electrodes. The current will melt the metals clamping material together without excessive heating of other areas of the component, flowing through the spot welding electrodes in a very short time (from ten to one hundred milliseconds). Referring to honeycomb structured components, the tack-welding process is usually used in Avio to temporarily clamp this type of component to other aero-engine components and next to join them together in the brazing process. In practice, the tack-welding process is used as fixture for brazing. The quality of the brazing process is strictly dependent on the previous tack-welding process. Each time that brazed junctions are rejected the cause is always due to tack-welding operation. Before experimental activities, tack-welding process was still a manual process in Avio therefore it was much affected by factory worker's skill. In fact the automating of tack-welding process is very hard to realize due to several process parameters to manage and set. The "trial & error" strategy, frequently used in industry, is not able to solve this kind of problem.

Therefore, in order to make the process automatic, the aims of this task, summarized in the attached *Paper II*, were:

1. to characterize the tack-welding process, that is to detect which factors affect the quality of brazed joint between the honeycomb and the other component;
2. to determine the optimum setting of the tack-welding process parameters.

METHODOLOGICAL APPROACH

The experimental study is divided in two phases: screening and optimization. Following the systematic approach to planning for a designed industrial experiment proposed in Coleman and Montgomery (1993) and Ilzarbe at al. (2008), and just successfully applied in Avio Palumbo (2009), two pre-design sheets (i.e. main and secondary sheets) were conceived and implemented. As mentioned above, these two kinds of sheets force the experimenter to address fundamental questions since the early phase of the experimental activities and, moreover, they enable him to record the results of the interaction between statistical and technological competences during face-to-face discussion.

In the first screening experimental phase the following control factors are adopted: energy sector (A), firing force (B), width (C), squeeze time (D) and hold time (E). Factors A and C are welding-pulse parameters and represent the amount of heat (energy) delivered to the spot in a pulse and the weld time during which welding current is applied to the metal surfaces, respectively. Factor B is the force squeezing the metal work-pieces' surfaces to be joined together. Factor D is the time interval between the initial application of the electrode force on the work-piece and the first application of current, while factor E is the time, after the welding, when the electrodes are still applied to the sheet to chill the weld. Note that, before the systematic and team driving experimental activity described in *Paper II*, the factors D and E had never been modified by Avio.

The quality of tack-welding process is evaluated only after brazing by a certified inspector able to check the following geometrical and metallurgical parameters: (I) cell geometry (i.e. amount of distorted or bended cells); (II) integrity of brazing alloy layer (i.e. lack of material or uniformity in brazing alloy layer between honeycomb and the other brazed component); (III) detachment of the central part (i.e. amount of cells not well-brazed in the central zones); detachment of the peripheral parts (i.e. amount of cells not well-brazed in the upper (IV) or lower (V) zones of the honeycomb). These response variables are evaluated along the component surface using a microscope with different zoom degrees depending on the particular response variable. The certified inspector adopts a visual rating system for each response variable. It consists of a scale from 0 to 5, where 5 is the most desirable value and 0 is unacceptable. Before starting the screening experimental phase a training period of a whole month for the inspector involved in the visual rating evaluation has been conceived.

In the pre-experimental phase a 2^{5-1} design is adopted. For each treatment three replications have been executed, for a total of 48 experimental runs. The ANOVA method is applied in order to test the statistical significance of main effects and two-factor interactions for each one of the five chosen response variables.

The two-factor interaction DE (squeeze time-hold time), for integrity of brazing alloy layer (II), and mainly the two factor interactions DE and AE (energy sector-hold time), for cell detachment in the upper part (IV), are the true “discoveries” of this first screening experimental phase. In fact, these interactions involve the factors D (squeeze time) and E (hold time) about which, until now, little was known in Avio about their potential use; moreover these interactions are of anti-synergic type and therefore the practitioner, even though expert in tack-welding process, would never have been able to anticipate this type of interaction during the pre-experimental phase.

On the basis of the results obtained in the first screening experimental phase, in the second optimization phase a three-variable (A, D and E) CCD with three center points is adopted. For each treatment two replications have been executed, for a total of 34 experimental runs.

It is not very unusual in the industrial field to have several process responses that need to be simultaneously optimized as it happens in tack-welding process. The problems related to develop a strategy in order to jointly optimize more than one response simultaneously are known as multi-response optimization (MRO) problems. There are several methods proposed in the literature for solving MRO problems. In *Paper II* a solution, based on the desirability function method introduced in Derringer (1980), is proposed.

Results obtained were very relevant in both improvement of the tack-welding process, and the improvement of company’s confidence in the statistics as tool for innovation. Before experimental activities. Finally, the obtained results in the research activity have enabled the company to properly set the automatic tack-welder machine, keeping met all geometrical and metallurgical requirements, and to increase productivity. In fact, adopting the optimal parameter setting in production context the percentage of well-brazed honeycomb structure components has increased from 82% to 98%.

PAPER II

A systematic approach to process improvement via Design of Experiments: a case study in tack-welding process

De Chiara G.[1], Marrone R.[1], Palumbo B.[2], Tagliaferri F.[2]

[1] AVIO S.p.A., Manufacturing Technologies Department, Pomigliano d'Arco, Naples, Italy, gaetano.dechiara@aviogroup.com.

[2] University of Naples Federico II, Department of Aerospace Engineering, P.le Tecchio 80, 80125 Naples, Italy, biagio.palumbo@unina.it.

Abstract

Tack-welding is a very common process in aero-engine manufacturing companies. It is usually used in AVIO to temporarily clamp honeycomb structured components to other aero-engine components and next to join them together in the brazing process. The quality of the brazing process is strictly dependent on the previous tack-welding process. The aims of this paper are: 1) to characterize the tack-welding process, that is to detect which factors affect the quality of brazed joint between the honeycomb and the other component; 2) to determine the optimum setting of the tack-welding process parameters. The experimental study is divided in two phases: screening and optimization. In this phase a systematic approach to planning for designed industrial experiment has been proposed. In this way statistical and technological knowledge are fully involved in the experimental activities. In order to jointly optimize more than one response simultaneously a solution based on the desirability function method has been proposed.

Keywords: design of experiment, tack-welding process, desirability function.

1 INTRODUCTION

Based on previously experimental activities [1] there is enough awareness in AVIO about the strategic role that a systematic and sequential approach to industrial experimentation plays in technological process improvement [2]. In order to integrate engineering and statistical knowledge and to put into action a virtuous cycle of sequential learning [3] [4], consistent with Six Sigma approach [5], more emphasis has to put on action in the pre-experimental phase were statistical and technological competencies must be fully exploited.

As highlighted in [6] the pre-experimental phase lays the experimental foundations of the successive screening and optimization phases.

In the first experimental phase (screening) the objective is to characterize the tack-welding process, that is to detect which factors affect the quality of brazed joint between the honeycomb and the other component.
In the second phase (optimization) the aim is to determine the optimum setting of the tack-welding process parameters. All experiments were carried out in a production context.
This is a paper in which both statistical and technological aspects are involved. The statistical methodologies applied in the experimental phases are extensively treated in the literature [7] and so they will be applied without any explicit introduction or analytical formulation. The case study involving tack-welding process has been developed by the AVIO industry, an aerospace company at the leading edge of propulsion technology.

2 TECHNOLOGICAL CONTEXT AND APPLICATIVE CASE STUDY

Tack-welding is a very common process in aero-engine manufacturing companies like AVIO. Referring to honeycomb structure component, it is usually used in AVIO to temporarily clamp this type of component to other aero-engine components and next to join them together in the brazing process.
The quality of the brazing process is strictly dependent on the previous tack-welding process. Each time that brazed junctions are rejected the cause is always due to tack-welding operation.
The quality of tack-welding process is evaluated only after brazing by a certified inspector able to check the following geometrical and metallurgical parameters, Figure 1: (a) cell geometry (i.e. amount of distorted or bended cells); (b) integrity of brazing alloy layer (i.e. lack of material or uniformity in brazing alloy layer between honeycomb and the other brazed component); (c) detachment of the central part (i.e. amount of cells not well-brazed in the central zones); (d) detachment of the peripheral parts (i.e. amount of cells not well-brazed in the upper or lower zones of the honeycomb).
At the present time tack-welding process is still a manual process in AVIO and so it is deeply affected by factory worker's skill.
Before starting with the experimental activities the average percentage of well-brazed honeycomb structure components was about 82%. The aim of Manufacturing Technologies Department is to increase it.

3 PRE-EXPERIMENTAL PHASE

Following the systematic approach to planning for a designed industrial experiment proposed in [6], and just successfully applied in AVIO [1], two pre-design sheets (i.e. main and secondary sheets) were conceived and implemented.

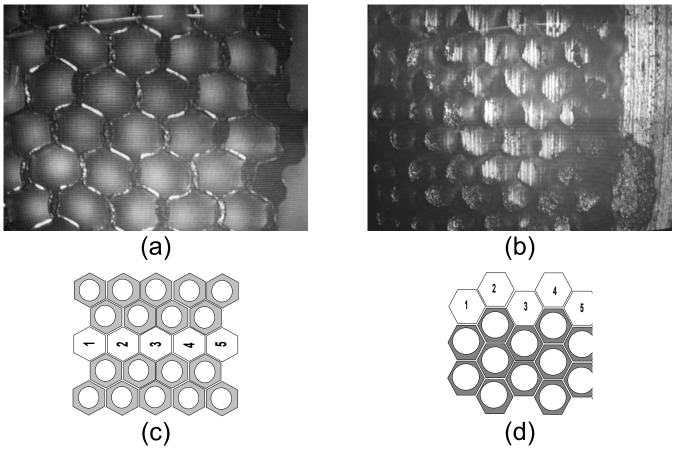

Figure 1. Main metallurgical and geometrical defects associated with a tack-welded and later brazed honeycomb structure component: (a) cell geometry; (b) integrity of brazing alloy layer; (c) detachment of the central part; (d) detachment of the peripheral parts

These two kinds of sheets force the experimenter to address fundamental questions since the early phase of the experimental activities and, moreover, they enable him to record the results of the interaction between statistical and technological competences during face-to-face discussion. These sheets are the only official document circulating among the team involved in the experimentation.

The main sheets contain information about the objective of the experimentation, the relevant background, the response variables and the factors (i.e. control, held-constant and nuisance factors).

The secondary sheets deepen the technological relationship between control factors and response variables, in terms of expected main effects and interactions. Cell geometry (I), integrity of brazing alloy layer (II), detachment of the honeycomb's central part (III), detachment of the honeycomb's marginal upper part (IV) and lower part (V) are the response variables taken in consideration. These variables are measured by a certified inspector who score them.

In the first screening experimental phase the following control factors are adopted: energy sector (A), firing force (B), width (C), squeeze time (D) and hold time (E). Factors A and C are welding-pulse parameters and represent the amount of heat (energy) delivered to the spot in a pulse and the weld time during which welding current is applied to the metal surfaces, respectively. Factor B is the force squeezing the metal work-pieces' surfaces to be joined together. Factor D is the time interval between the initial application of the electrode force on the work and the first application of current, while factor E is the time, after the welding, when the electrodes are still applied to the sheet to chill the weld.

Note that, before the systematic and team driving experimental activity described in this paper, the factors D and E had never been modified by AVIO. We reduce the influence of the operator and of other factors, which cannot be controlled from a technological or economical point of view, by planning and implementing a well-studied manufacturing procedure in order to conduct a more meaningful experimental activity.
The tack-welding experiments were performed on an automatic Unitek-Miyachi tack-welder machine (customized by AVIO), using a unique pattern of spot weld in terms of total number of delivered spots and delivery scheme. Each spot in the experiments was welded through only a pulse, as usually occurs in the production field given the high number of spots carried out to realize a welded joint.

4 SCREENING PHASE

4.1 Experimental design

In the pre-experimental phase a 2^{5-1} design is adopted. This design, with I=ABCDE (defining relation), is a resolution V design, thus enables one to obtain reliable information about main effects and two-factor interactions.
Table 1 summarizes the levels of control factors and their settings. Table 2 shows the 2^{5-1} design matrix. For each treatment three replications have been executed, for a total of 48 experimental runs. In order to reduce the disturbance of any unconsidered noise factor, the order of trials is randomized both in the treatments and in their replications.

Control factors	Labels	Low (-)	High (+)	Unit
Energy sector	A	50	90	%
Firing force	B	156	356	N
Width	C	SHORT	MEDIUM	---
Squeeze time	D	0,15	2,0	sec
Hold time	E	0,5	2,0	sec

Table 1. Control factors and their settings

The response variables are evaluated along the component surface using a microscope with different zoom degrees depending on the particular response variable. The certified inspector adopts a visual rating system for each response variable. It consists of a scale from 0 to 5, where 5 is the most desirable value and 0 is unacceptable. Before starting the screening experimental phase a training period of a whole month for the inspector involved in the visual rating evaluation has been conceived.

Treatment	A	B	C	D	E = ABCD
1	-	-	-	-	+
2	+	-	-	-	-
3	-	+	-	-	-
4	+	+	-	-	+
5	-	-	+	-	-
6	+	-	+	-	+
7	-	+	+	-	+
8	+	+	+	-	-
9	-	-	-	+	-
10	+	-	-	+	+
11	-	+	-	+	+
12	+	+	-	+	-
13	-	-	+	+	+
14	+	-	+	+	-
15	-	+	+	+	-
16	+	+	+	+	+

Table 2. Table of plus and minus signs for the 2^{5-1} design (defining relation I=ABCDE)

4.2 Analysis of results

The ANOVA method is applied in order to test the statistical significance of main effects and two-factor interactions for each one of the five chosen response variables. The model diagnostic checking has been successfully performed, via graphical analysis of residuals. Pareto charts of standardised effects (α=0.05) have been elaborated and analyzed. The experimental results for all five responses, in terms of main effects and two-factor interactions, are summarized in Table 3.

Terms	I	II	III	IV	V	Terms	I	II	III	IV	V
A						AE				x	
B	x					BC					
C	x	x	x	x	x	BD					
D						BE					
E						CD					
AB						CE	x			x	
AC					x	DE		x		x	
AD				x							

Table 3. Significant main effects and two-factor interactions

The two-factor interaction DE (squeeze time-hold time), for the integrity of brazing alloy layer (II), and the two factor interactions DE and AE (energy sector-hold time), for the cell detachment in the upper part (IV), are the true “discoveries” of this first screening experimental phase. In fact, these interactions involve the factors D (squeeze time) and E (hold time) about which, until now, little was known in AVIO about their potential use; moreover, these interactions are of anti-synergic type (Figure 2) and therefore the practitioner, even though expert in tack-welding process, would hardly have been able to anticipate this type of interaction during the pre-experimental phase.

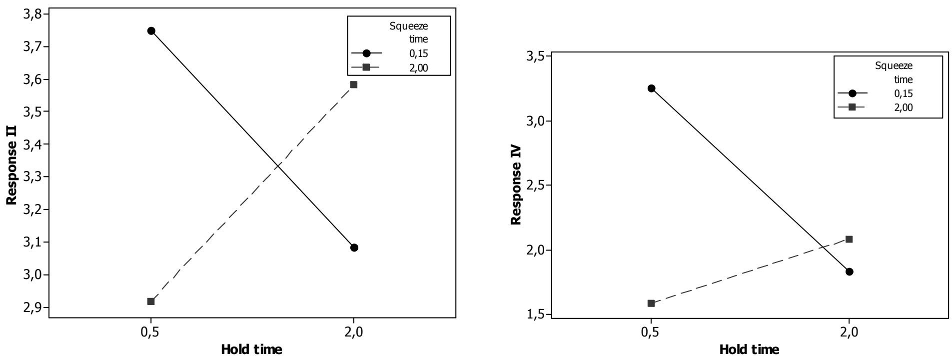

(a) (b)

Figure 2. Anti-synergic interactions: (a) DE for integrity of brazing alloy layer (II); (b) DE for cell detachment in the upper part (IV)

4.3 Technological interpretation of results

The technological interpretation of results developed in this screening phase is very important and enables obtaining information potentially useful for the next optimization phase. Width (C) is a significant (α=0.05) factor on all responses. All response variables are higher in value when C is at a “low” level (short).

Width (C) is strictly related to the weld time, that is, time during which welding current is applied to the welded parts. Choosing a width as short as possible is strategic to control wearing of the electrodes which could be one of the main causes of honeycomb’s detachments (III, IV and V) and distorted cells (I). The information acquired in the screening phase about the factor C will enable us to set it “low” (short) in the next optimization phase.

Firing force (B) and all two-factor interactions involving it are not significant (α=0.05) on almost all the response variables. It is significant only on the cell geometry (I).

However, because this output variable is not the most critical response for the overall quality of the process, this factor will be excluded in the next experimental phase.
In order to reduce cell geometry defects, best results can be obtained setting firing force (B) "high" (356 N).
From a welding technical point of view, two-factor interactions involving squeeze time (D) and hold time (E) are the most interesting results of this experimental phase. The significance of their anti-synergic interactions on some output variables, and in particular on the responses IV and V, the most critical responses for a good quality of the process, explains the great difficulties that AVIO's tack-welding specialists/technologist always met in dealing with their settings.
Observing interaction plots (Figure 2), it is clear that in terms of integrity of brazing alloy layer (II) best results can be obtained either setting both hold time (E) and squeeze time (D) at their low level or setting hold time and squeeze time at their high level.
The choice of the first setting, useful also in terms of cell detachment in the upper part (IV), is preferable both in terms of electrode life and manufacturing cycle time. In fact, hold time (E) is necessary to allow the weld nugget to solidify before releasing the welded parts, but it must not be too long as this may cause the heat in the weld spot to spread to the electrode and heat it. Similar effects can be caused by setting a too long squeeze time.
Such working conditions allow electrode wearing process to be faster so that a good quality of the process can be also reached by adopting high levels for squeeze and hold time only in the case of a very frequent change of the electrode itself. This possibility does not really match with the company's needs.

5 OPTIMIZATION PHASE

5.1 Experimental design and desirability function

It is not very unusual in the industrial field to have several process responses that need to be simultaneously optimized as it happens in tack-welding process. The problems related to develop a strategy in order to jointly optimize more than one response simultaneously are known as multi-response optimization (MRO) problems. There are several methods proposed in the literature for solving MRO problems [8] [9] [10]. In this paper we adopt the procedure proposed in [8].
The first step for the experimenter is to transform each response Y_i $(i=1,2,\dots,5)$ into an individual response of desirability d_i $(0\leq d_i\leq 1\ i\ i=1,2,\dots,5)$.
In practice a desirability function transforms each response variable onto a [0,1] scale where 1 is the most desirable value and 0 is unacceptable.
The desirability function d_i adopted in this case study comes from the one-sided-desirability transformation proposed in Derringer and Suich (1980). The function d_i increases as the response Y_i increases and the target is to maximize the response itself. Results:

$$d_i = \begin{cases} \left(\dfrac{Y_{i,max} - Y_i}{Y_{i,max} - Y_{i,min}} \right)^r & Y_{i,min} \le Y_i \le Y_{i,max} \\ 0 & \text{otherwise} \end{cases} \quad (1)$$

where *r* is a weight that can be assigned to change the shape of the desirability transformation.

In order to simultaneously optimize all the responses Y_i, the second step is to combine the individual desirability d_i in an overall desirability function *Df*. Several methods are available in the literature [9]. In this paper we adopt the multiplicative method proposed in [8]. Results:

$$Df = \left(d_1^{w_1} \times d_2^{w_2} \times \ldots \times d_5^{w_5} \right)^{1 / \sum_{i=1}^{5} w_i} \quad (2)$$

where the response weights w_i are shown in Table 4.

Response variables	Labels	Desirability d_i	Weights w_i
Cell geometry	I	d_I	2
Integrity of brazing alloy layer	II	d_{II}	1
Cell detachment in the central part	III	d_{III}	3
Cell detachment in the upper part	IV	d_{IV}	4
Cell detachment in the lower part	V	d_V	4

Table 4. Response weights

In the screening phase the factors A, D and E (see Table 1) result significant on response variables taken into consideration. Therefore, in the optimization phase a three-variable, Central Composite Designs (CCD) with three center points is adopted. Table 5 summarizes the levels of control factors and their settings.

Table 6 shows the CCD (α=1) matrix. For each treatment two replications have been executed, for a total of 34 experimental runs and the order of trials is randomized both in the treatments and in their replications as in the previous experimental phase.

Control factors	Labels	Low (-)	Medium (0)	High (+)	Unit
Energy sector	A	50	70	90	%
Squeeze time	D	0,15	1,075	2,0	sec
Hold time	E	0,0	0,5	1,0	sec

Table 5. Control factors and their settings

Treatment	A	D	E	Treatment	A	D	E
1	-1	-1	-1	9	-α	0	0
2	-1	-1	1	10	α	0	0
3	-1	1	-1	11	0	-α	0
4	-1	1	1	12	0	α	0
5	1	-1	-1	13	0	0	-α
6	1	-1	1	14	0	0	α
7	1	1	-1	15	0	0	0
8	1	1	1	16	0	0	0
				17	0	0	0

Table 6. CCD with α=1 (Face-Centered Cube)

Finally such an overall desirability function *Df* has been optimized to identify the best setting for the control factors. In this case study, the objective of step (v) is to maximize *Df*. In this way the multivariate optimization problem changes into a univariate one.

5.2 Analysis of results and their technological interpretation

Statistical analysis of data was done by using Minitab® statistical package version 15. The results in terms of multiple response desirability with separate models are shown in Figure 3.

The maximum composite desirability is 0.793. This value allows the experimenter to understand the level of the parameters where the maximum of overall desirability function *Df* occurs. It is interesting to evaluate how the overall desirability function *Df* fluctuates for small changes in control parameters as, for example, the squeeze time (D) and the hold time (E).

In order to deepen these aspects, Figure 4shows the contour plots of the overall desirability function *Df* for the three possible pairs of control factors (AD, AE, DE), with factors firing force (B) and width (C) set at “high” levels (356 N) and “low” (short), respectively. These plots show that, except for the energy sector (A), small departures from optimality of both the squeeze time (D) and hold time (E) values are possible without causing a high decrease in overall desirability function *Df*.

The decision to explore the region of the domain around the maximum point for the squeeze time (D) was taken by the team work since the “optimum” found by the overall desirability function *Df* does not allow us: i) to achieve a very high value in terms of honeycomb’s cell detachment in the upper part (IV), which is one of the most important responses; ii) to have a short manufacturing cycle time.

So, in order to take into account these specific technological requirements, slight deviations from the optimum level of both squeeze time (D) and hold time (E) have been adopted.

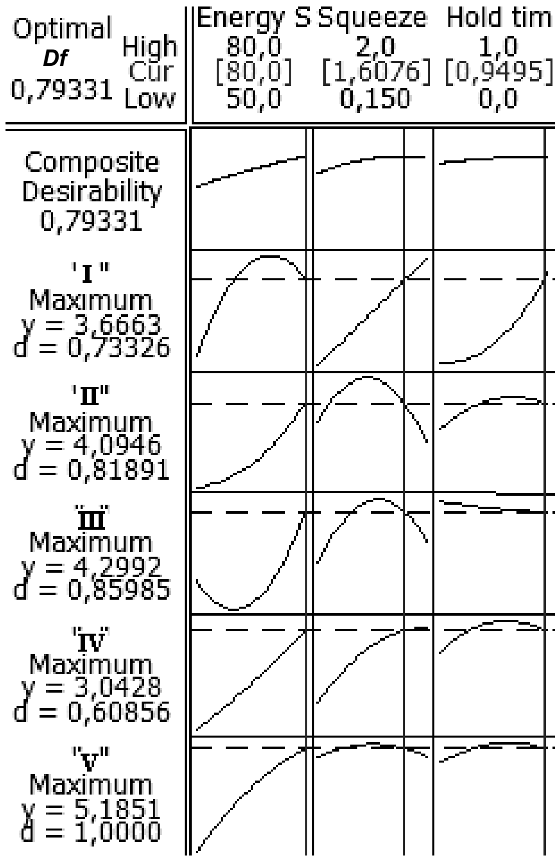

Figure 3. Multiple response desirability with separate models

The final setting adopted in production context is shown in Table 7. Many tests were carried out adopting this final setting. The results confirmed high values of the overall desirability function *Df*.

Adopting the new parameter setting in production context the percentage of well-brazed honeycomb structure components has increased from 82% to 98%.

6 CONCLUSION

This paper has showed the strategic role that a systematic approach to planning for a designed industrial experiment plays in technological process innovation as well as the great efficacy that a desirability function analysis can offer the industrial experimenter in dealing with MRO problems.
The team approach is the real driving force of pre-experimental activities; it enables us to integrate engineering and statistical knowledge and catalyze the process innovation and, moreover, it allows us to put into action a virtuous cycle of sequential learning.

The results obtained in the first screening experimental phase have allowed us to understand which factors affect the quality of a honeycomb's brazed joint, made by a pre-brazing tack-welding process, in terms of five geometrical and metallurgical outcomes. Moreover, the technological interpretation of results has allowed practitioners to gain technological knowledge that, together with an approach based on the desirability analysis, has been very useful for achieving the results in the next phase.

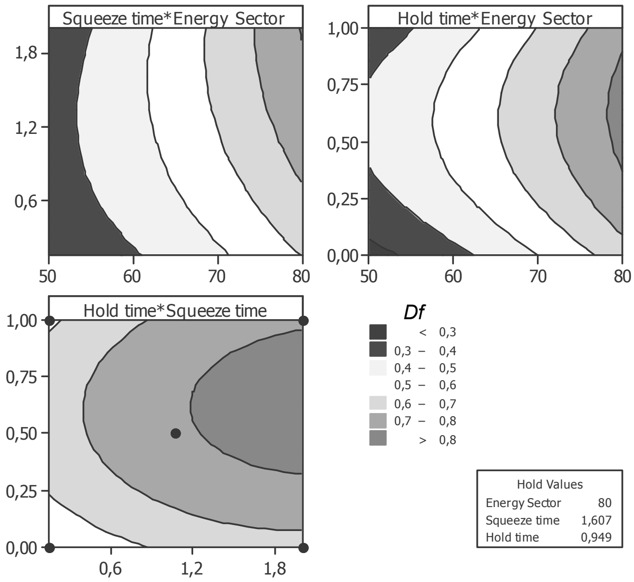

Figure 4. Contour plots of the overall desirability function *Df* for the three pairs of control factors (AD, AE, DE)

Control factors	Labels	Level	Unit
Energy sector	A	80	%
Firing force	B	356	N
Width	C	SHORT	---
Squeeze time	D	1.2	sec
Hold time	E	0.5	sec

Table 7. Optimal settings of control factors

The results obtained in the second optimization experimental phase have enabled the company to properly set the automatic tack-welder machine, to keep meeting geometrical and metallurgical requirements reaching a very high overall quality and to increase productivity.

REFERENCES

[1] Palumbo, B., Marrone, R., De Chiara, G., 2009. Technological process innovation via engineering and statistical knowledge integration, Erto (Ed.), Statistics for Innovation, Statistical design of continuous product innovation, Springer, pp. 177-190.

[2] Ilzarbe, L., Álvarez, M.J., Viles, E., Tanco, M., 2008. Practical applications of design of experiments in the field of engineering: a bibliographical review, Quality and Reliability Engineering International, vol. 24(4), pp. 417-428.

[3] Box, G., 2001: Statistics for discovery, Journal of Applied Statistics, vol. 28(3-4), pp. 285-299.

[4] Deming, W.E., 1982. Out of crisis, Cambridge University Press, Cambridge.

[5] Montgomery, D.C., Woodal, W.H., 2008. An overview of six sigma, International Statistical Review, vol. 76(3), pp. 329-346.

[6] Coleman, D.E., Montgomery, D.C., 1993. A systematic approach to planning for a designed industrial experiment, Technometrics, vol. 35(1), pp. 1-12.

[7] Montgomery, D.C., 2005. Design and analysis of experiment, Wiley, New York.

[8] Derringer, G., Suich, R., 1980. Simultaneous optimization of several response variables, Journal of Quality Technology, vol. 12(4), pp. 214-219.

[9] Kros, J.F., Mastrangelo, C.M., 2001. Comparing methods for the multi-response design problem, Quality and Reliability Engineering International, vol. 17(2), pp. 323-331.

[10] Fogliatto, F., 2008. Multiresponse optimization of products with functional quality characteristics, Quality and Reliability Engineering International, vol. 24(1), pp. 927-939.

STATISTICAL CHARACTERIZATION AND OPTIMIZATION OF LASER DRILLING ON NICKEL SUPERALLOY

The following case study has been developed in the Pomigliano d'Arco (Naples) site, Avio Group's Centre of Excellence for combustors, reheats and combustion systems production.

TECHNOLOGICAL CONTEXT

Over the last years the laser micro-drilling of some critical components, as the Heat Shields and the Screech Damper (assembled on reheat of the EJ200 engine), has been the focus of some projects and research collaborations developed along with DIAS (Department of Aerospace Engineering, University of Naples "Federico II"). Those components, manufactured on nickel based superalloy C263, are characterized by thousands of micro-holes, arranged in parallel lines (see *Figure 4*). In fact the system of cooling (effusion cooling) is constituted by a series of small diameter holes, called *effusion holes*, that cross the reheat wall. The air flows, from a part draining heat crossing the wall, from the other, forms an air film on the hot zone protecting it from the action of warm gases. Obviously the effusion holes are necessary to decrease the heat stress proper of warm components of the engines. There are many effusion hole typologies, different for axis tilt angle on workpiece surface, diameter, machined thickness, etc

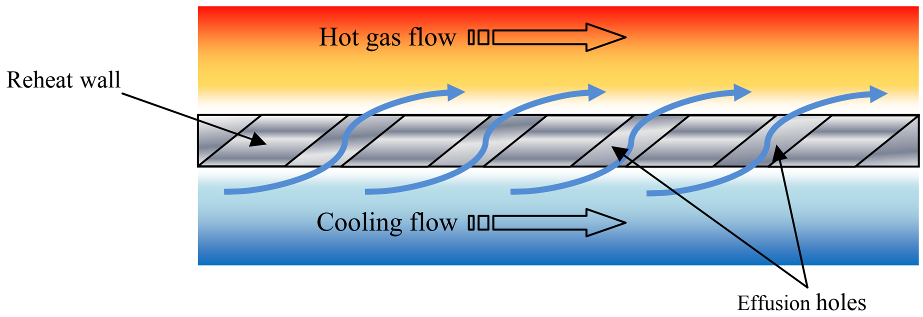

Figure 4 Effusion cooling system

In aerospace industry, laser drilling is the most economical process for drilling many thousands of high quality effusion holes with a small diameter in order to improve the cooling capacity of the engine components, such as blades, combustion chambers or reheats.

Three different laser drilling methods are usually used to obtain these holes: percussion, trepanning and drilling on the fly (DOF). The first one consists in cutting the circumference of the hole all around. The percussion method makes the hole by shooting several times the place to drill, without a relative motion between laser and workpiece.

In the DOF method, the laser pulses are delivered to the workpiece while it is rotating around its own axis; the rotation of the part is synchronized with the laser pulse (or shots), ensuring that multiple pulses are always delivered to the exact position of the hole, so that the hole is created after a fixed number of workpiece rotations. The DOF method is better than the other ones in terms of productivity because it allows an important process time reduction, but it is not always better in terms of the quality of the hole.

High productivity and high quality hole are the competitive key factors for industries involved in laser drilling processes. The quality of the hole is related to several geometrical and metallurgical parameters: taper (i.e. non-cylindrical nature of the hole), barrelling (i.e. irregular depressions on the hole side-wall), recast layer (i.e. material accumulated on the hole side-wall), spatter (i.e. re-solidified material at the entrance of the hole), dross (i.e. re-solidified material at the exit of the hole).

The achievement of optimum quality of the hole during laser drilling is one of the most important issues in this specific research area. Several parametric studies aiming to study the relationship between laser parameters and hole quality characteristics, for different several aerospace materials, are available in scientific literature; in particular, Ghoreishi et al. (2002) and (2007), Yeo et al. (1994), Bandyopadhyay et al. (2002) and Dubey and Yavada (2008).

A few year ago, the Manufacturing Technology Department of Avio fixed as a main target to find the best working parameters set to drill by DOF method, in order to obtain an increase in productivity. The collaboration with the research group on "Statistics, Quality and Reliability" of DIAS, and the origin of a research team, composed by Avio's qualified figures and academic staff, allowed to fix in the center the main target, in accordance with aeronautical specification.

Recently, a new experimental campaign has been developed, in order to further enhance laser drilling process productivity. This time, the increase of productivity was set down as reduction of number of laser shots needed to drill, in accordance with technical specifications. The team was encouraged by the belief that the attainments of this objective would have led for both components to a significant decrease of process time: more than 25% for the selected holes.

EXPERIMENTAL DESIGN AND SET-UP

The key to success was the statistical approach. Even this time, following the systematic approach to planning for a designed industrial experiment proposed in Coleman and Montgomery (1993) and Ilzarbe at al. (2008), and just successfully applied in Avio Palumbo (2009), two pre-design sheets (i.e. master and supplementary sheets) were conceived and implemented. We customize the proposed guide sheets in order to make them more appropriate and comprehensive in the specific technological context. These sheets were the only official document circulating among the team involved in the experimentation.

Laser drilling experiments were performer by 250W Nd:YAG laser emitting at a wavelength of 1.063 μm with a fixed beam delivery. The laser beam was approximately 14 mm in diameter; it was focused with a 200 mm focal length lens, giving a spot size of approximately 0.47 mm diameter (M^2 value of ~24). Oxygen assist gas was used due to the results of previous experimentation. Each experiment was performed through a conical copper nozzle with 1.15 mm diameter orifice, and the beam was always inclined at 30° to the surface, as this configuration was identified by Avio as being the one that is the most critical to this process. The reheats component thicknesses and the hole diameter (less than a millimeter) are omitted here for industrial confidentiality reasons.

The response variables chosen were: taper, alpha and beta angles and the recast layer thickness. Taper is measured as the difference between *beta* angle and *alpha* angles, as shown in *Figure 5*. Theoretically, for a hole, if the taper angle value is zero and the hole axis perfectly oriented, both alpha and beta angles will be alike the impact angle of laser beam on the workpiece surface. This value (i.e. impact angle of laser beam) is the target for alpha and beta angles. The recast layer thickness are measured on the hole's borders, as shown in *Figure 6*.

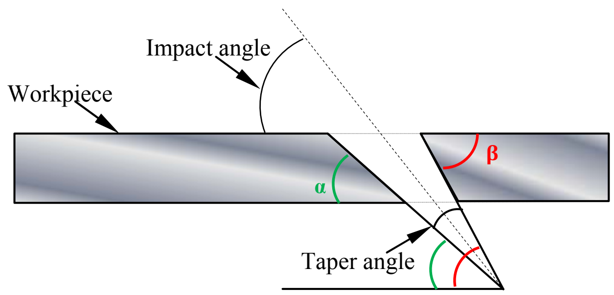

Figure 5 Measurement of taper (beta - alpha)

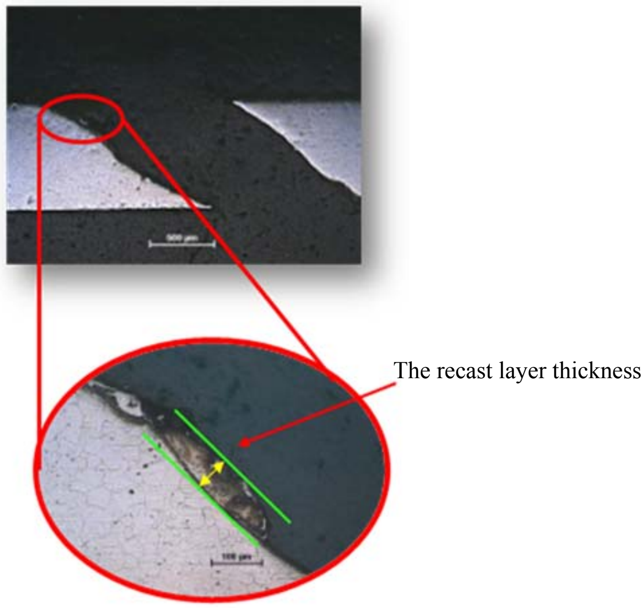

Figure 6 The recast layer thickness

All variables are measured in the hole section, by an expert laboratory operator, using a microscope with different zoom degrees. Therefore, the quality control test for laser drilled micro-holes, in terms of taper and recast layer thickness, is a destructive test. Consequently, all the experiments are carried out on a cylinder artifact made of the same material as the reheats.

On the basis of preliminary tests, the following process parameters were chosen as control factors: peak power (A) on 3 levels, laser beam pulse width (B) on 2 levels, assist gas pressure (C) on 2 levels and defocus (D) on 2 levels.

Defocus (distance between the laser focal spot and the workpiece surface, see *Figure 7*) plays a key role in the drilling process. In fact its modulation is set to obtain a hole of the diameter desired through the laser beam divergence effect.

Making a reduction of laser beam pulse numbers to realize every hole, the loss of energy due to defocus of the beam becomes crucial. Therefore a new drilling strategy was implemented and tested: the use of a variable defocus (see *Figure 7*) between two different shots to limit energy loss due to laser beam divergence effect.

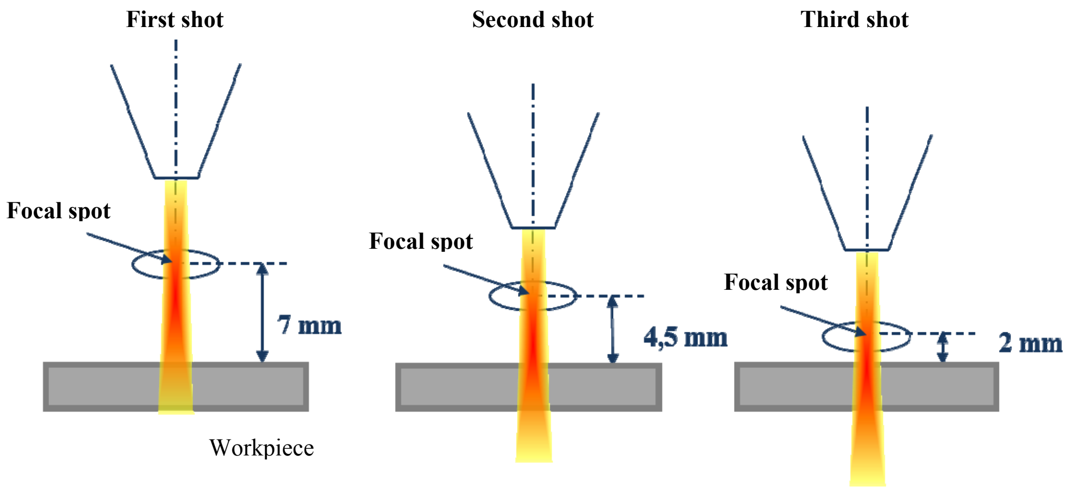

Figure 7 Variable defocus

Generally, in a factorial design, the experimental region, has a regular shape. The experimental region results from product of all factor ranges and is regular when it is like a cube in *n*-dimensions (where *n* is the number of factors involved).

Due to technological constraints, an irregular experimental plan was chosen to use selecting factor levels of pulse width related to peak power level. This strategy has the advantage to extend the experimental region in order to make appreciable the effects on the response variables. This choice has been done because peak power and pulse width factors are related to each other; in fact there is a physical link that connects them: *Energy = peak power * pulse width*. So, at the same energy for each peak power level, the value of pulse width is determinate; at least two different energy levels was selected, 20 J and 24,5 J (see *Figure 8*).

Due to the specific experimental condition, a *nested-factorial design* was chosen. *Table 4* summarizes the levels of control factors and their settings.

Table 5 shows the nested-factorial design matrix. For each treatment two replications have been executed, for a total of 48 experimental runs, performed following a randomized run order.

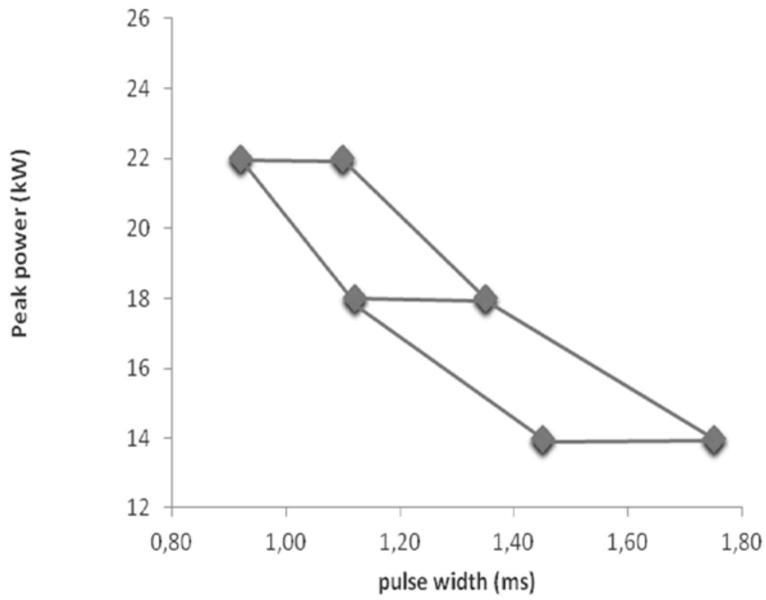

Figure 8 Relationship between peak power and pulse width

		B(A): Pulse width	
	A: Peak Power	-1	+1
+1	22 kW	0,92 ms	1,1 ms
0	18 kW	1,12 ms	1,35 ms
-1	14 kW	1,45 ms	1,75 ms
	C: Pressure		
+1	12 bar		
-1	7 bar		
	D: Defocus		
+1	Variable Defocus		
-1	Normal Defocus		

Table 4 Levels of control factors and their settings

Treatment	Peak power A	Pulse width B(A)	Pressure C	Defocus D
1	-1	-1	-1	-1
2	-1	1	-1	-1
3	1	-1	-1	-1
4	1	1	-1	-1
5	-1	-1	1	-1
6	-1	-1	-1	1
7	-1	-1	1	1
8	-1	1	-1	1
9	-1	1	1	-1
10	-1	1	1	1
11	1	-1	1	-1
12	1	-1	1	1
13	1	-1	-1	1
14	1	1	-1	1
15	1	1	1	-1
16	1	1	1	1
17	0	-1	-1	-1
18	0	-1	-1	1
19	0	-1	1	-1
20	0	-1	1	1
21	0	1	-1	-1
22	0	1	-1	1
23	0	1	1	-1
24	0	1	1	1

Table 5 Design matrix

ANALYSIS OF RESULTS AND TECHNOLOGICAL INTERPRETATION

The nested ANOVA method was applied in order to test the statistical significance of main effects and two-factor interactions for the response variable. The analysis was carried out at significance level of α=0.05. Following, only some of the significative factor effects, having a clear technological interpretation, were extensively discussed. The ANOVA tables for recast layer, alpha and beta, are reported in *Table 6*, *Table 7* and *Table 8* respectively.

Analysis of Variance for Recast layer

Source	DF	SS	MS	F	P
A	**2**	**4548,3**	**2274,1**	**4,20**	**0,025**
B(A)	**3**	**8271,3**	**2757,1**	**5,09**	**0,006**
C	1	6,0	6,0	0,01	0,917
D	1	285,2	285,2	0,53	0,474
A*C	2	76,0	38,0	0,07	0,932
A*D	2	1565,4	782,7	1,45	0,252
C*B(A)	3	271,1	90,4	0,17	0,918
D*B(A)	3	4223,6	1407,9	2,60	0,071
C*D	1	1598,5	1598,5	2,95	0,096
Error	29	15694,6	541,2		
Total	47	36540,0			

S = 23,2636 R-Sq = 57,05% R-Sq(adj) = 30,39%

Table 6 Nested ANOVA table for recast layer

Analysis of Variance for Alpha

Source	DF	SS	MS	F	P
A	**2**	**36,192**	**18,096**	**4,16**	**0,024**
B(A)	3	35,804	11,935	2,74	0,061
C	**1**	**36,208**	**36,208**	**8,32**	**0,007**
D	**1**	**28,310**	**28,310**	**6,51**	**0,016**
A*C	2	21,563	10,782	2,48	0,102
A*D	2	9,159	4,580	1,05	0,362
C*B(A)	3	8,394	2,798	0,64	0,594
D*B(A)	3	13,679	4,560	1,05	0,386
C*D	**1**	**45,448**	**45,448**	**10,45**	**0,003**
Error	29	126,178	4,351		
Total	47	360,936			

S = 2,08590 R-Sq = 65,04% R-Sq(adj) = 43,34%

Table 7 Nested ANOVA table for alpha

Analysis of Variance for Beta

Source	DF	SS	MS	F	P
A	**2**	**11,5128**	**5,7564**	**6,03**	**0,006**
B(A)	**3**	**11,5737**	**3,8579**	**4,04**	**0,016**
C	1	0,0105	0,0105	0,01	0,917
D	1	0,2788	0,2788	0,29	0,593
A*C	**2**	**23,6322**	**11,8161**	**12,37**	**0,000**
A*D	2	0,0053	0,0026	0,00	0,997
C*B(A)	**3**	**9,0337**	**3,0112**	**3,15**	**0,040**
D*B(A)	3	6,4258	2,1419	2,24	0,104
C*D	1	1,1545	1,1545	1,21	0,281
Error	29	27,6976	0,9551		
Total	47	91,3249			

S = 0,977287   R-Sq = 69,67%   R-Sq(adj) = 50,85%

Table 8 Nested ANOVA table for beta

Statistical analysis of data were done by using Minitab® statistical package version 15.

The technological interpretation of results is a very important phase. In fact, a check between technological "expectations", elicited in the pre-experimental phase, and the statistical results allows practitioners to gain technological knowledge and understand the added value of a systematic approach to planning for a designed industrial experiment. In fact, a positive check strengthens the trust level of practitioners in experimental activities; a negative check forces the practitioners to deepen the technological interpretation of results.

The presence of recast layer along internal walls of the holes is mainly caused by the physics of material removal that takes place during laser drilling. Recast layer thickness depends especially on the speed of removal and the amount of melting material generated during laser drilling.

Drilling with peak power (A) set at high level and pulse width (B(A)) set at low level, is preferable in order to obtain smaller recast layers, *Figure 9*. The heat surge of material, due to a sudden temperature load caused by a high energy laser pulse induced from a high peak power (A) and low pulse width (B(A)), causes, in fact, vaporization of the most part of removed material and thus a smaller amount of recast material on walls of drilled holes.

Therefore the recast layer thickness decreases with increasing of the peak power (A) and increases with increasing of the pulse width (B(A)), as expected. The recast layer thickness is not conditioned significatively by other factors. This kind of result consolidates the knowledge base of the company and reassures the experimenters about the reliability of the executed tests.

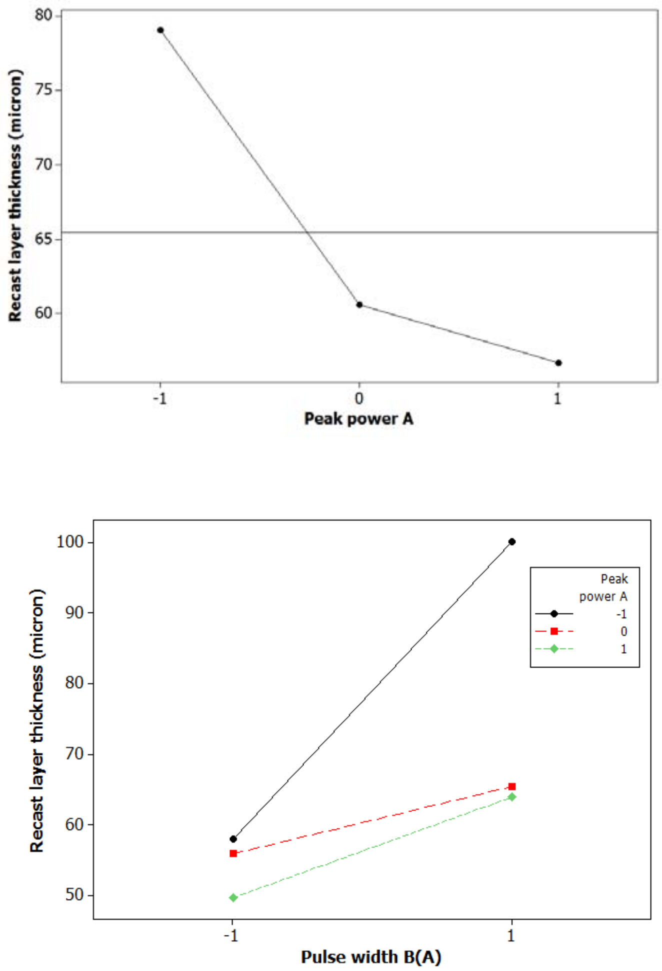

Figure 9 Main effects plots for recast layer thickness

In laser drilling the hole taper is often related to two main concurrent physic phenomena of material erosion: *crater-generator* and *beam-divergence* effects. The first one occurs on the higher layers of the drilled workpiece, while the second one is typically localized on the lower layers, where laser beam usually loses its power both of penetration and ablation because of its natural divergence.

As mentioned above, for the first time in Avio, alpha and beta angles have been analyzed separately in order to evaluate the taper causes. The most interesting comments were made on alpha angle: power peak (A), assist gas pressure (C) and defocus (D) play an important role on this response variable.

As shown in the main effects plots, *Figure 10*, a low level setting of the peak power (A) is preferable in order to close alpha on target value (i.e. 30°) and at least reduce taper.

However the true "discoveries" of this experimental phase is the effectiveness of variable defocus strategy (note that variable defocus strategy is codifying as +1 level of defocus).

Drilling by variable defocus strategy is preferable in order to obtain better alpha angle value. Also, the interaction plot between defocus and pressure (*Figure 11*) shows that the variable defocus strategy is effective to obtain an alpha angle near to the target value, when the pressure value is high.

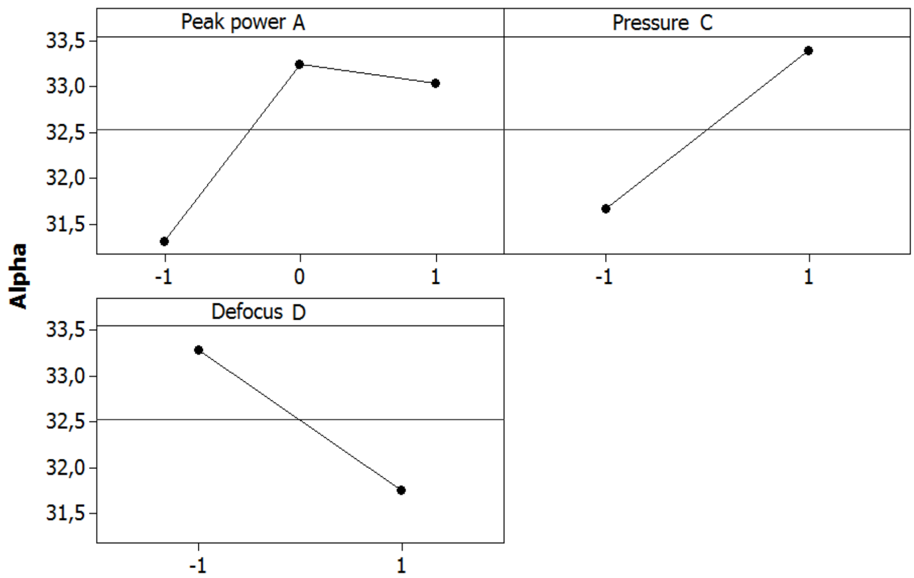

Figure 10 Main effect plots for alpha angle

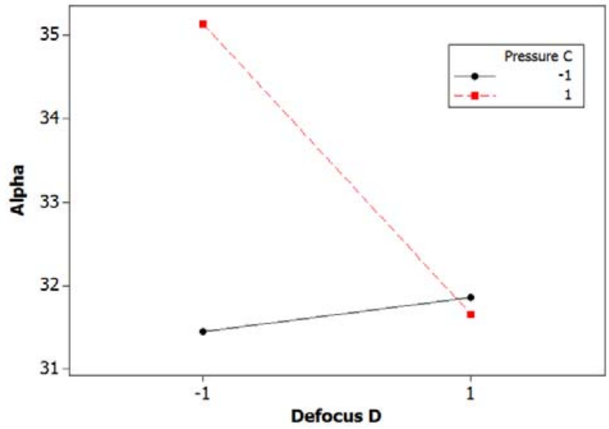

Figure 11 Interaction plot for alpha

Concerning beta angle, the main effects plot of peak power (A) shows that its intermediate level returns the more distant value from the target (see *Figure 12*). It is due to both beam-divergence and crater-generator effects.

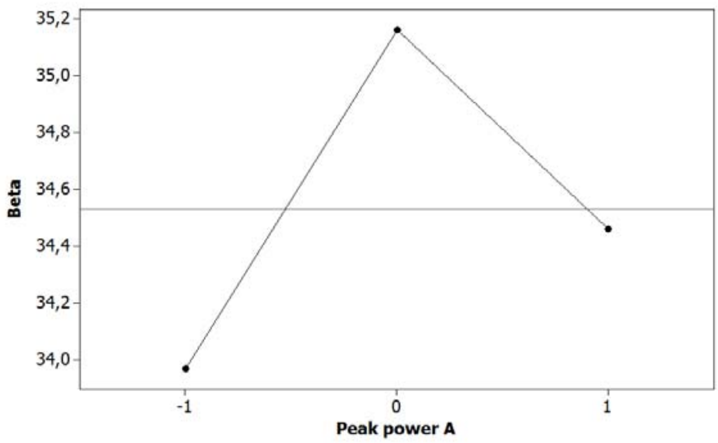

Figure 12 Main effect plot for beta

Crater-generator effect develops at the entry section of the beam and it is due to the laser beam insisting on the entry section of the hole for a long time and with major intensity compared to the exit section. The released energy at the hole entry section is major and this leads to a major removal of material. With the same energy of the pulse, the crater is the most evident, the higher is the peak power. This effect has also influence on alpha angle measure, but lesser by axis tilt angle of the hole on workpiece surface. (Note that, when peak power increases, crater-generator effects increases consequently beta angle increases too).

For these reasons main effect plot of peak power (A) for beta was the outcome of two opposite phenomena: crater-generator and beam-divergence effects.

Figure 13 shows, qualitatively, what has just been mentioned.

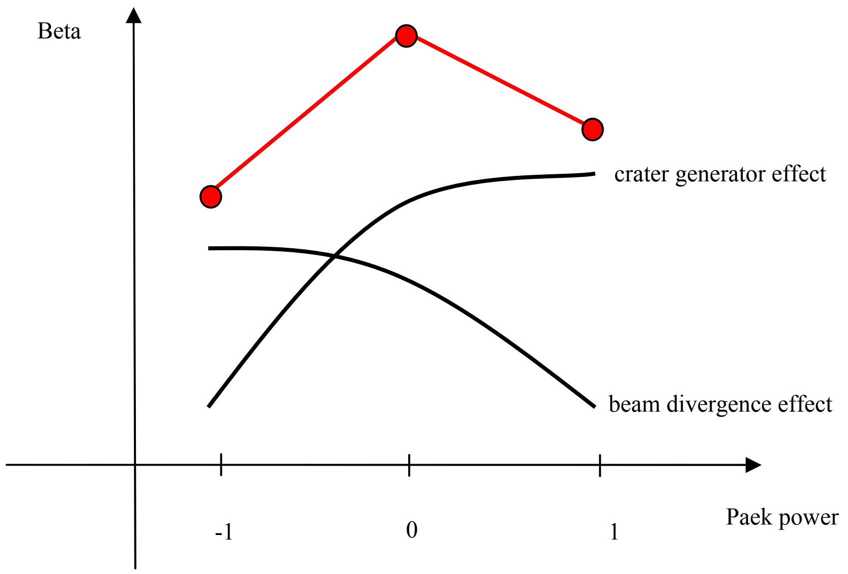

Figure 13 Main effect of peak power as outcome of crater-generator and beam-divergence effects

MAIN RESULTS OBTAINED

A systematic approach based on DoE allows to increase the process productivity (due to the reduction of process time) in a few tests (i.e. 48 tests performed); although optimal set of process parameters has not yet been found, but 16 sets of parameters, to drill in specific conformity, were identified. The best set to qualify for production, may be chosen among them.

The knowledge of laser micro-drilling DOF process on nickel based superalloy was increased, highlighting the links between machined parameters and the selected response variables (i.e. recast layer and the taper, the last one through the characterization of the alpha and beta angles).

The Nested ANOVA methodology allowed first the design of an experimental plan that "would fit" to the region of interest, conditioned by technological constraints, and then the detection of the significative effects ($\alpha=0.05$) of all factors including those related to each other.

Other new for the company, introduced by this work, is the choice of alpha and beta angles analysis instead of taper.

This innovation allowed first to characterize these angles and to deduce the physical and thermodynamic phenomena that affect them; second to find information about tilt angle of the hole (i.e. tilt angle between hole axis and workpiece surface) and its relation with process parameters.

More, the validity of the variable defocus method (innovative method for the company) has been tested; it has good influence on the alpha angle, thus indirectly on the hole taper.

This work, finally, is food for thought given the many ideas that could be explored in future; particularly:

1. to evaluate the impact of variable defocus strategy, on the quality features, as the defocus pattern changes;
2. to extend experimentation to other category of hole;
3. to study thoroughly and classify the causes of process noise of laser micro-drilling DOF trying to limit such causes through robust design.

CONCLUSION AND REMARKS

The results obtained in the three applicative examples discussed have shown the strategic role that a systematic approach to planning for a design of experiments plays in technological process innovation.

To improve the use of this technique, it is necessary to find the means of bringing together statistical concepts and practical knowledge in technical areas such as material science or mechanical engineering.

The first case study presented has been focused on the laser engraving of the Ti6Al4V alloy by means of a Q-Switched 30W Yb:YAG fiber laser. The results obtained in a first screening experimental phase enabled the factors that affect the depth of the machined volume and the quality of the machined surface in terms of roughness. In addition, experimental results have shown that, for each adopted pulse frequency, the machined volume linearly depends on the total amount of released energy. At last the best treatments in terms of roughness and machined removal rate have been evaluated too.

The second applicative example presented has handled the characterization and the optimization of tack-welding process. The results obtained in the first screening experimental phase have allowed us to understand which factors affect the quality of a honeycomb brazed joint, made by a pre-brazing tack-welding process, in terms of five geometrical and metallurgical outcomes. Moreover, the technological interpretation of results has allowed practitioners to gain technological knowledge that, together with an approach based on the desirability analysis, has been very useful for achieving the results in the next optimization phase.

The results obtained in the second optimization experimental phase have enabled the company to properly set the automatic tack-welder machine, to keep meeting geometrical and metallurgical requirements reaching a very high overall quality and to increase productivity.

The third applicative example presented has dealt with the micro-drilling of two components assembled on reheat of the EJ200 aero-engine. The aim of Manufacturing Technologies Department of Avio was to find the best working parameters set to drill by DOF method, in order to obtain an increase in productivity. Due to the results obtained, the knowledge of laser micro-drilling DOF process on nickel based superalloy was increased, highlighting the links between machined parameters and the selected response variables (i.e. recast layer and the taper, the last one through the characterization of the alpha and beta angles). Although optimal set of process parameters has not yet been found, but 16 sets of parameters, to drill in specific conformity, were identified. The best set to qualify for production, may be chosen among them. More, the validity of the variable defocus method (innovative method for the company) has been tested; it has good influence on the hole taper.

ACKNOWLEDGEMENTS

The author is particularly grateful to Avio Industry and CIRTIBS Research Centre, for providing the equipments and their resources to develop the present research work.

REFERENCES

Bandyopadhyay S, Sundar JKS, Sundararajan G, Joshi SV. *Geometrical features and metallurgical characteristics of Nd:YAG laser drilled holes in thick IN718 and Ti–6Al–4V sheets*. Journal of Materials Processing Technology, Vol. 127, 2002, pp. 83-95.

Box GEP, Hunter JS, Hunter WG. *Statistics for Experimenters -Design, Innovation and Discovery* (2nd edn) (Wiley Series in Probability and Statistics). Wiley: New York, 2005.

Box GEP. *Statistics for discovery*. Journal of Applied Statistics, Vol. 28(3-4), 2001, pp. 285-299.

Cheng WS, Wu CFJ, Huwang L. *Statistical modeling for experiments with sliding levels*. Institute of Mathematical Statistics, Lecture Notes-Monograph Series Vol. 52, 2006, pp. 245-256.

Chryssolouris G. *Laser Machining - Theory and Practice*. Mechanical Engineering Series, Springer-Verlag, New York Inc., NewYork, 1991.

Cicală E, Soveja A, Sallamand P, Grevey D, Jouvard JM. *The application of the random balance method in laser machining of metals*. Journal of Materials Processing Technology, Vol. 196, 2008, pp. 393-401.

Coleman DE, Montgomery DC. *A systematic approach to planning for a designed industrial experiment.* Techometrics, Vol. 35, No. 1, 1993, pp. 1-12.

Costa NRP, Pires AR, Ribeiro CO. *Guidelines to help practitioners of design of experiments.* TQM Magazine Vol. 18(4), 2006, pp. 386-399.

Czitrom V. *One factor at a time versus designed experiments*, Amer. Statist. Vol. 53(2) 1999, pp. 126-131.

Del Castillo E, Montgomery DC, McCarville DR. *Modified desirability functions for multiple response optmization*. Journal of Quality Technology, Vol. 28(3), 1996, pp. 337-345.

Deming WE. *Out of crisis*. Cambridge University Press, Cambridge, 1982.

Derringer G, Suich R. *Simultaneous optimization of several response variables*. Journal of Quality Technology, Vol. 12(4), 1980, pp. 214-219.

Derringer G. *A balancing act: Optimizing a product's properties*. Quality Progress, Vol. 27(6), 1994, pp. 51-58.

Dubey K, Yadava V. *Laser beam machining - A review*. International Journal of Machine Tools & Manufacture, Vol. 48, 2008, pp. 609-628.

Duley WW. *CO2 Laser: Effect and applications*, Academy Press, New York, 1977.

Erto P. *Probabilità e statistica per le scienze e l'ingegneria*. Mcgraw-Hill, 2008.

Fogliatto F. *Multiresponse optimization of products with functional quality characteristics*. Quality and Reliability Engineering International, Vol. 24(1), 2008, pp. 927-939.

Genna S, Leone C, Lopresto V, Santo L, Trovalusci F. *Study of fiber laser machining of C45 steel: influence of process parameters on material removal rate and roughness*. International Journal of Material Forming, Vol. 3/1, 2010, pp. 1115-1118.

Ghoreishi M, Low DKY, Li L. *Comparative statistical analysis of hole taper and circularity in laser percussion drilling*. International Journal of Machine Tools & Manufacture, Vol. 42, 2002, pp. 985–995.

Ghoreishi M, Nakhjavani OB. *Optimisation of effective factors in geometrical specifications of laser percussion drilled holes*. Journal of Materials Processing Technology, Vol. 196, 2007, pp. 303-310.

Hahn GJ, *Experimental Design in the Complex World.* Technometrics Vol. 26, No. 1, 1984, pp. 19-31.

Harrington EC. *The desirability function*. Industrial Quality Control, Vol. 21, 1965, pp. 494-498.

Harry MJ. *The Vision of Six Sigma: A Roadmap for Breakthrough*. Sigma, Phoenix, 1994.

Ilzarbe L, Álvarez MJ, Viles E and Tanco M. *Practical applications of Design of Experiments in the field of engineering: abibliographical review*. Quality And Reliability Engineering International, Vol. 24, 2008, pp. 417-428.

Kaldos A, Pieper HJ, Wolf E, Krause M. *Laser machining in die making-a modern rapid tooling process*. Journal of Materials Processing Technology, Vol. 155-156, 2004, pp. 1815-1820.

Kim KJ, Lin DKJ. *Optimization of multiple responses considering both location and dispersion effects*. European Journal of Operational Research, Vol. 169, 2006, pp. 133-145.

Kros, JF, Mastrangelo CM. *Comparing methods for the multi-response design problem*. Quality and Reliability Engineering International, Vol. 17(2), 2001, pp. 323-331.

Leone C, Morace RE, De Iorio I. *AISI 304 Stainless Steel Engraving by Q-Switched Nd:YAG Nanosecond Laser.* Journal of the Chinese Society of Mech. Eng., Vol. 28 No.2, 2007, pp. 217-224.

Lorenz A, Emmelmann C. *Methodical investigations for increasing process capability of short pulse laser ablation in high precision die and mould industry*. High-Power Laser Ablation VI. In: Proc. of SPIE, 6261, 626122, 2006.

Marrone R. *Industrial skill advance via design of experiments: a case study of an international competition*. Doctorate Thesis, 2009.

Meijer J. *Laser beam machining (LBM), state of the art and new opportunities*. Journal of Materials Processing Technology, Vol. 149, 2004, pp. 2-17.

Montgomery DC, Woodal WH. *An overview of six sigma*. International Statistical Review, Vol. 76(3), 2008, pp. 329-346.

Montgomery DC. *Design and Analysis of Experiments*. Wiley: New York, 2005.

Montgomery DC. *Experimental design for product and process design and development*. The Statistician, Vol. 48 No. 2, (1999) pp. 159-77.

Myers RH, Montgomery DC. *Response Surface Methodology: Process and Product* Optimization Using Designed Experiments. John Wiley & Sons, New York, 1995.

Palumbo B, Marrone R, De Chiara G. *Technological process innovation via engineering and statistical knowledge integration*. Erto P (Ed.), Statistics for Innovation, Statistical design of continuous product innovation, Springer, 2009, pp. 177-190.

Pande PS, Neuman RP, Cavanagh RR. *The Six Sigma Way: How GE, Motorola, and Other Top Companies are Honing Their Performance*. McGraw Hill: New York, 2000.

Ribardo C, Allen TT. *An Alternative Desirability Function for Achieving 'Six Sigma' Quality*. Quality and reliability engineering international, Vol. 19, 2003, pp. 227-240.

Taguchi G. *Sistem of experimental design*. Unipub/Kraus International Publications, White Plins, New York, 1987.

Tanco M, Viles E, Álvarez MJ, Ilzarbe L. *Why is not design of experiments widely used by engineers in Europe?*. Journal of Applied Statistics Vol. 37, No. 12, 2010, pp. 1961–1977.

Wu CFJ, Hamada M. *Experiments*. Wiley/Interscience: New York, 2000.

Yeo CY, Tam SC, Jana S, Lau MWS. *A technical review of the laser drilling of aerospace materials*. Journal of Materials Processing Technology, Vol. 42, 1994, pp. 15-49.

ATTACHMENTS

ATTACHMENT I:

TECHNICAL REPORT - Laser Assisted Milling of nickel based alloys

Technical Report

Topic:	LAM (Laser Assisted Milling) of nickel-based alloys (Nicrofer® 5923 hMo - alloy 59)
Organization:	Technische Universität Chemnitz
Testing objectives:	To know the parameters influence due to maximize productivity. At elevated temperatures, the mechanical properties change, with yield strength decreasing and the material deformation behavior changing from brittle to ductile, thus reducing tool wear, improving surface finish and increasing material removal rates. The feasibility of the method and its advantages have been proved through the application of LAM to difficult-to-machine metals.

ACTIVITIES

TASK	SUB-TASK	DETAILS	STATUS
Pre-design			
	Literature review	An extensive review of international literature was performed	**Performed**
	Selection of response variables	The following response variables are selected: **F_x [N]; F_y [N]; F_z [N]; VB; SKV; MRR** (for details see attached pre-design guide sheets)	**Performed**
	Choice and definition of parameters	The following control factor are selected: **a_p; f_z; v_c.** (for details see attached pre-design guide sheets)	**Performed**
	Definition of factor value ranges for testing (min-max)	The following control factor are selected: **a_p:** [..] ÷ [..] **f_z:** [..] ÷ [..] **v_c:** [..] ÷ [..] (for details see attached pre-design guide sheets)	**Performed**

Prepared by:
F. Tagliaferri
DIAS–Università degli Studi di Napoli, Federico II

Rev. A
20/10/2011

TASK	SUB-TASK	DETAILS	STATUS
Definition of design			
	choice of appropriate design of experiment	The chosen plan are full factorial design 2^3 for 3 replications (for details see attached pre-design guide sheets)	**Performed**
	use of specialized software to plan test's order	By use of Design Expert Software (trial version)	**Performed**
Tests		The tests were completely performed in 2 days	**Performed**
Laboratory analysis			
	wear measure	Not performed yet	In progress
	force's diagrams	Not performed yet	In progress
Statistical Analysis		Not performed yet	In progress
Technological interpretation of results		Not performed yet	In progress
Publication of results		Not performed yet	In progress

Pre-design guide sheets

GENERAL DATA

Responsible for testing:	
Organization:	Technische Universität Chemnitz
Topic:	LAM (Laser Assisted Milling) of nickel-based alloys (Nicrofer® 5923 hMo - alloy 59)
Testing objectives: (also in terms of response variables target values) should be unbiased, specific, measurable, and of practical consequence	To know the parameters influence due to maximize productivity. At elevated temperatures, the mechanical properties change, with yield strength decreasing and the material deformation behavior changing from brittle to ductile, thus reducing tool wear, improving surface finish and increasing material removal rates. The feasibility of the method and its advantages have been proved through the application of LAM to difficult-to-machine metals.

To remember:

	Steps of experimentation
1	**Recognition of and statement of the problem**
2	**Selection of the response variable(s)**
3	**Choice of factors and levels**
4	**Choice of experimental design**
5	Conduction of the experiment
6	Data analysis
7	Conclusions and recommendations

	Pre-design Guide Sheets	
1	Name, Organization, Title	
2	Objectives	
3	Relevant Background and Equipment	
4	Response Variables/Factors	Focus on supplem. sheets
5	Control Variables/Factors	
6	Factors to be "held constant"	
7	Nuisance factors	
8	Interactions	
9	Restrictions	
10	Responsibility for coordination	
11	Design preferences	
12	Analysis and presentation techniques	
13	Trial run?	

Prepared by:
F. Tagliaferri
DIAS–Università degli Studi di Napoli, Federico II

Checked by:
A. Rößler / D. Hösel
TU-Chemnitz

BACKGROUND

Relevant helpful results and information (on response and control variables) from previous experience, physical law, theoretical relationships, paper, specialist opinions, expert knowledge:

n°**1**	**Source/reference:** Brecher C., Rosen C., Emonts M. - Laser-assisted Milling of Advanced Materials – Physics Procedia 00 (2010) 000-000 **Helpful information for testing:** Aiming the reduction of process forces, increased material removal rates and longer tool service life without application of cooling lubricants the Fraunhofer IPT has developed a novel process concept for laser-assisted milling with local laser-induced material plastification before cutting. The thermally induced loss of material strength significantly increases the machinability concerning the achievable material removal rates or formability and tool service life. Conventional milling without laser-assistance produced large flaking at the insert edge whereas the laser-assisted process revealed only little edge and flank wear. The laser spot is not positioned peripheral to the cutting zone but directly projected onto the cutting surface of the respective chip volume inducing local material plastification before cutting.
n°**2**	**Source/reference:** Alauddin M., El Baraide M.A., Hashmi M.S.J. - Modeling of cutting force in end milling Inconel 718 - J. of Material Processing Technology 58 (1996) 100-108 **Helpful information for testing:** A high cutting force is generated in machining lnconel 718 (nickel-base alloy). This paper presents a study of the development of a mathematical model for average tangential cutting force in end milling lnconel 718 using uncoated carbide inserts under dry conditions. The predictive cutting force model has been developed in terms of cutting speed and axial depth of cut by response surface methodology. Response surface contours were constt ucted in feed-axial depth of cut planes by a computer. The model was tested by analysis of variance and found to be adequate. In order to estimate the model parameters of the equation an orthogonal first-order design was used, The orthogonal first-order design of experiment (with two factors: fz [mm/z]; ap [mm]) consists of nine experiments.
n°**3**	**Source/reference:** Mark Anderson, Rahul Patwa, Yung C. Shin - Laser-assisted machining of Inconel 718 with an economic analysis - International Journal of Machine Tools & Manufacture 46 (2006) 1879–1891

	Helpful information for testing: Laser-assisted machining (LAM) offers the ability to machine superalloys more efficiently and economically by providing the local heating of the workpiece prior to material removal by a single point cutting tool. The machinability of Inconel 718 under varying conditions is evaluated by examining tool wear, forces, surface roughness, and specific cutting energy. With increasing material removal temperature from room temperature to 620 1C, the benefit of LAM is demonstrated by a 25% decrease in specific cutting energy, a 2–3-fold improvement in surface roughness and a 200–300% increase in ceramic tool life over conventional machining. Moreover, an economic analysis shows significant benefits of LAM of Inconel 718 over conventional machining with carbide and ceramic inserts. The tool during LAM still appears to fail by notch wear, but as the average material removal temperature increases, the notch wear of the tool decreases. The average flank wear during LAM is significantly lower than conventional machining, but increases as temperature increases suggesting that a maximum beneficial temperature may be achieved before the tool rapidly fails by flank wear. The wear and chipping on the secondary face do not appear to limit tool life as temperature increases. Specific cutting energy decreases significantly during LAM from conventional machining, but shows little change at material removal temperatures between 360 and 540 °C.
n°4	**Source/reference:** Wu X F, Wang Y, Zhang H Z - System Design for Laser Assisted Milling of Complex Parts - Proceedings of the 36th International MATADOR Conference 2010, 18, 577-580, DOI: 10.1007/978-1-84996-432-6_126 http://www.springerlink.com/content/k055151636p73028/ **Helpful information for testing:** Laser assisted milling (LAML) is a potential method for machining difficult-to-machine materials such as superalloys and ceramics. Several LAML experiments have showed the feasibility of the method and advantages including good surface finish, decreased cutting force and tool wear, and no large microcrack zones. The material removal temperature is the key parameter influencing machining results. At elevated temperatures, the mechanical properties change, with yield strength decreasing and the material deformation behavior changing from brittle to ductile, thus reducing tool wear, improving surface finish and increasing material removal rates.
n°5	**Source/reference:** Laura Ilzarbe, María Jesús Álvarez, Elisabeth Viles and Martín Tanco - Practical Applications of Design of Experiments in the Field of Engineering: A Bibliographical Review - Quality And Reliability Engineering International 2008; 24:417–428 Published online 19 February 2008 inWiley InterScience (www.interscience.wiley.com). DOI: 10.1002/qre.909 **Helpful information for testing:** The design of experiments (DoE) methodology is a technique that has been applied for many years in industry to improve quality. In this study, a summary of 77 cases of practical DoE application in the field of engineering is presented.

Analytical relationships between the different process parameters:		Legend:

1. $a_e \approx (0{,}3 \div 0{,}25) * D$ for "hard" materials	**2.** $f = f_z * Z$	a_e = contact width *(radial depth of cut)*;
		D = tool diameter;
		f = feed rate per rotation; *(avanzamento a giro)*
		f_z = feed per tooth; *(avanzamento del dente)*
		Z = number of teeth/cutting isert number;
		n = rotation speed;
		v_c = cutting speed;
		V = voleme;
		a_p = infeed *(radial depth of cut)*;
		s = milling length;
		v_f = feed rate; *(avanzamento a minuto)*
		MRR = material removal rate;
		φ_s = cut-bend-angle.

3. $n = {}^{v_c}/_{(\pi * D)}$	**4.** $V = a_e * a_p * s$	
5. $v_f = f_z * Z * n$	**6.** $MRR = a_e * a_p * v_f$	
7. $\varphi_s = 2 * \arcsin\left({}^{a_e}/_{D}\right)$		

EQUIPMENT

1.

Tool: ATI Stellram 7690VA 12 SA025Z3R35 Modular Head

7690 VA 12 Modular Head/Screw-on

EDP #	Part Number	D	L/H	M	d_1	a_p max.	No. of Inserts	EDP# (Spares)	Spares	EDP# (Spares)	Spares	Screw tightening Nm
031106	7690VA 12 SA025Z3R35	25	35	M12	12.5	11	3	027860	F3007T	022157	T8	1,40

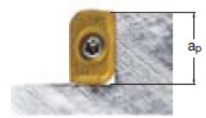

Depth of Cut (ap)

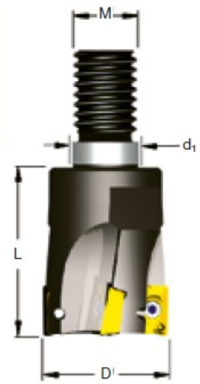

Modular Head

2. **Insert**: ADET 12 T308ER-48 SP6519 x500

Inserts for 7690 VA 12

EDP#	Part Number	Grade	Application & Material: Roughing ▼	Semi-Finishing ▼▼	Finishing ▼▼▼	Dimensions (mm): d	l	s	r	$h_m$min
030856	ADET 12 T308ER-48	X500	♦♦	♦♦		8,0	12,9	4,4	0.8	0,04

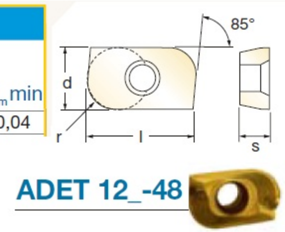

3. **Machine**: DMG | DECKEL MAHO | GILDEMEISTER - DMU 125 P duoBLOCK® | 5-axis machining
http://uk.dmg.com/en,milling,dmu125pduoblocknd?opendocument

4. **Diode Laser** OptoTools (nLIGHT) Continuous laser P_0=800W; λ=915÷980 nm (see also technical data sheet)
SW: SCAPS – Scanner application software

5. **Pyrometer:**
SW: LompocPro 6.0

6. **Axes force measurement system**: Kistler Multicomponent Dynamometer Typ 9255B (see also technical data sheet)
SW: LabView

7. **Microscope** ……….
SW: ………..

RESPONSE VARIABLE

Response Variable	**Target** (relationship of response variable to objective)	**Normal operating level and range** (currently)	**Measurement precision, accuracy How known?**
F_x [N] instantaneous feed component *(the projection of resultant cutting force in X direction)*	minimize (to reduce wear and needed power)	Unknown for the test material	Range: -20 ÷ 20 kN Calibrated partial range 0 ... 2 kN Threshold: <0,01 N from dynamometer data sheet
F_y [N] instantaneous normal component *(the projection of resultant cutting force in X direction)*	minimize (to reduce wear and needed power)	Unknown for the test material	Range: -20 ÷ 20 kN Calibrated partial range 0 ... 2 kN Threshold: <0,01 N from dynamometer data sheet
F_z [N] instantaneous vertical component *(the projection of resultant cutting force in X direction)*	minimize (to reduce wear and needed power)	Unknown for the test material	Range: -10 ÷ 40 kN Calibrated partial range 0 ... 4 kN Threshold: <0,01 N from dynamometer data sheet
VB [mm]	minimize (to increase the tool life)	Unknown for the test material	as per: IS0 3685:1993(E)
SKV [mm]	minimize (to increase the tool life)	Unknown for the test material	………………
MRR [cm^3/min]	Maximize (to increase the productivity)	Unknown for the test material	by formula

CONTROL FACTORS, HELD-COSTANT FACTORS, NOISE FACTORS

Factor	Control	Held-Constant	Noise	Why this choice? What is the alleged influence of the factor on the response variables?
Contact width $\mathbf{a_e}$ [mm] *(radial depth of cut)*		X		Previous experience and literature have shown that contact width has a low influence on the analyzed variables
Infeed $\mathbf{a_p}$ [mm] *(axial depth of cut)*	X			Previous experience and literature have shown that the infeed (and some of its interactions) have a high influence on the analyzed variables
Milling length **s** [mm]		X		It coincides with the workpiece length
Number of teeth/cutting edge number **Z**		X		It is the number of teeth (inserts) of the tool recommended in the catalog
Mode (laser assisted)		X		Previous experience and literature have shown that the laser use has a high influence on the analyzed variables. Due to the limited number of available inserts, this parameter is kept fixed
Tool diameter **D** [mm]		X		It is the diameter of the tool recommended in the catalog (ATI Stellram)
Feed per tooth $\mathbf{f_z}$ [mm/z]	X			Previous experience and literature have shown that cutting length per tooth has a high influence on the analyzed variables
Cutting speed $\mathbf{v_c}$ [m/min]	X			Previous experience and literature have shown that cutting speed has a high influence on the analyzed variables
Machined volume **V** [cm^3]	-	-	-	$= f(a_e, a_p, s)$
Feed rate per rotation **f** [mm/r]	-	-	-	$= f(f_z)$
Rotation speed **n** [rpm]	-	-	-	$= f(v_c)$
Feed rate $\mathbf{v_f}$ [mm/min]	-	-	-	$= f(f_z, n)$
Angle in action **κ** [°]		X		= *f*(tool geometry (insert & modular Head))
Cut-bend-angle $\boldsymbol{\varphi_s}$ [°]		X		$= f(a_e, D)$

Laser scanner speed $\mathbf{v_s}$ [mm/s]		**X**		50mm/s, to have a start parameter
Surface temperature **T** [°C]		**X**		500 °C because at elevated temperatures, the mechanical properties change as per ThyssenKrupp VDM Material Data Sheet No. 4030 *
				* (see Table 5 below)

Temperature (T) °C	°F	Yield strength [1] $R_{p0.2}$ N/mm²	ksi	$R_{p1.0}$ N/mm²	ksi	Tensile strength [2] R_m N/mm²	ksi	Elongation A_5 %
93	**200**		≥ 43		≥ 48		95 (91)	50
100	212	≥ 290		≥ 330		650 (620)		
200	392	≥ 250		≥ 290		615 (585)		
204	**400**		≥ 36		≥ 42		89 (85)	
300	572	≥ 220		≥ 260		580 (550)		
316	**600**		≥ 31		≥ 37		84 (80)	
400	752	≥ 190		≥ 230		545 (515)		
427	**800**		≥ 26		≥ 32		77 (74)	
450	842	≥ 175		≥ 215		525 (495)		

[1] For plates above 30 mm and up to 50 mm ($1^3/_{16}$ to 2 in.) thickness the yield strength values should be reduced by 20 N/mm² (3 ksi).
[2] Values for rods in brackets.

Table 5 – Mechanical properties at elevated temperatures according to VdTÜV data sheet 505 for thicknesses up to 30 mm ($1^3/_{16}$ in.).

CONSTRAINTS, LIMITATIONS AND RESTRICTIONS

1.	Only 20 insets are available.
2.	Reduced period of experimentation: from 1/8/2011 to 30/8/2011
3.	It is not possible to completely randomize the tests, you must first run the tests with the low level of the Infeed parameter ($\mathbf{a_p}$ -*axial depth of cut*) and then those with the highest level due to the workpiece geometry.

4. Workpiece dimensions [mm]:

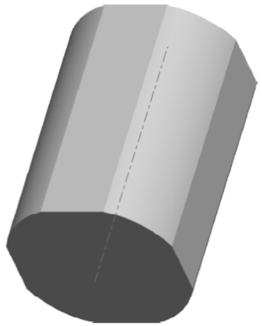

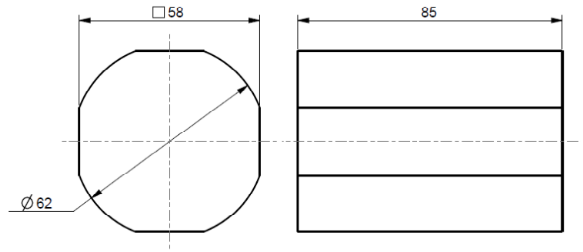

MODE AND TIPS TO BE TAKEN INTO EVIDENCE

1. The basic geometry of milling process:

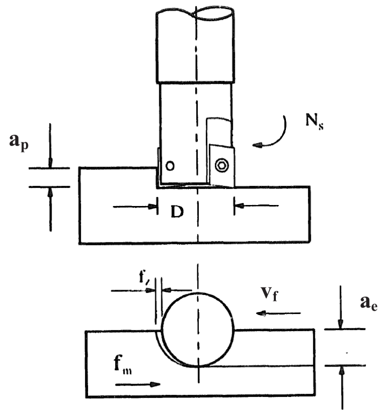

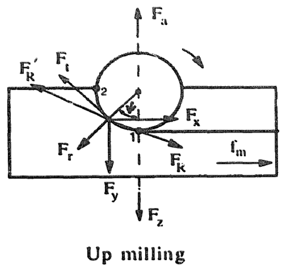

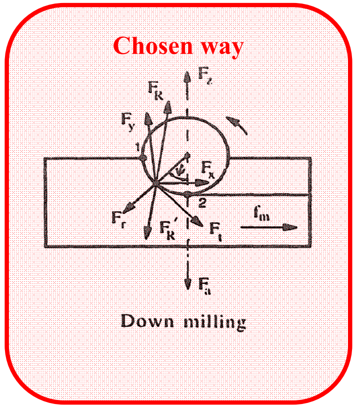

2. Each insert has 2 available cutting edges

3. About the milling tool course: 1 linearly course for each test

4. As per **IS0 3685:1993(E)**
(pages: 11÷13)

The criteria most commonly used for sintered carbide tools are as follows:

a) the maximum width of the flank wear land VB_B max. = 0,6 mm if the flank wear land is not regularly worn in zone B;

b) the average width of the flank wear land VB_B = 0,3 mm, if the flank wear land is considered to be regularly worn in zone B;

c) the depth of the crater KT given, in millimetres, by the formula

$$KT = 0{,}06 + 0{,}3f$$

where f is the feed expressed in millimetres per revolution.

For standard feeds, this leads to the values of KT given in table when KT applies as a criterion.

Feed f mm/rev.	0,25	0,4	0,63
Crater depth KT mm	0,14	0,18	0,25

Table - Values of KT

d) the crater front distance reduces to a value of KF = 0,02 mm;

e) the crater breaks through at the minor cutting edge, causing a poor finish of the machined surface.

NOTES

4 It should be recognized that notch wear is normally due to chemical action and occurs outside the area of physical contact between tool and workpiece both along the major cutting edge and to a lesser extent along the minor cutting edge. In both instances notch wear affects both the face and the flank simultaneously.

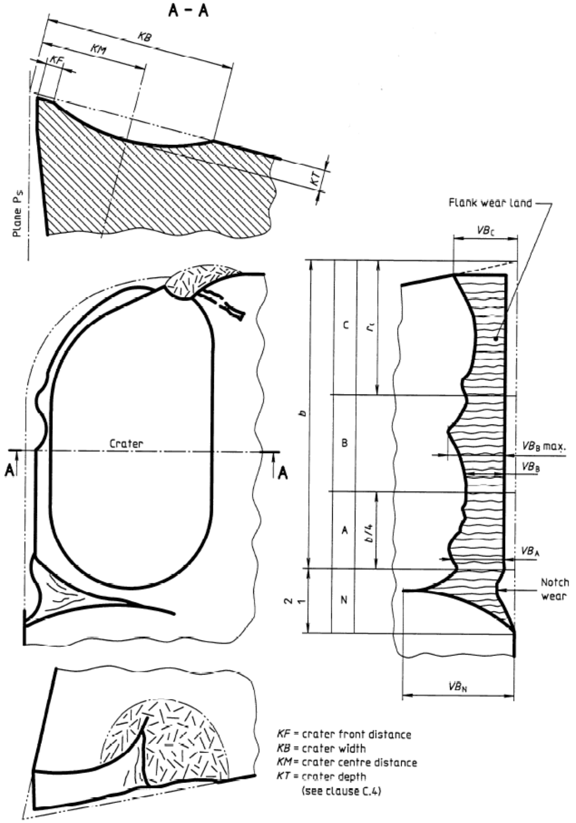

5 Notch wear, which in some cases can cause catastrophic failure , should be distinguished from abrasive wear VB_A which occurs along the cutting edge coincident with the work surface. Notch wear is often caused by work hardening effects in the workpiece by the previous pass of the tool.

8.3 Tool wear measurements

Particles adhering to the flank directly under the wear land can give the appearance of a larger width of the wear land. Also a deposit in the crater results in lower values of the crater depth. Loose material shall be removed carefully but chemical etchants shall not be used except at the end of the test.
For the purpose of the wear measurements, the major cutting edge is considered to be divided into four zones as shown in figure.
Zone C is the curved part of the cutting edge at the tool corner.
Zone B is the remaining straight part of the cutting edge between zone C and zone A.
Zone A is the quarter of the worn cutting edge length b farthest away from the tool corner.
Zone N extends beyond the area of mutual contact between the tool and workpiece for approximately 1 mm to 2 mm along the major cutting edge. The wear is of notch type.
The width of the flank wear land VB_B shall be measured within zone B in the tool cutting edge plane P_s[1]) perpendicular to the major cutting edge.
The width of the flank wear land shall be measured from the position of the original major cutting edge.
The crater depth KT shall be measured as the maximum distance between the crater bottom and the original face in zone B.
Further details are given in annex C.

[1] The tool cutting edge plane P, is the plane containing the major cutting edge and the assumed direction of primary motion.

RESPONSIBILITY FOR COORDINATION

What	Who

Prepared by:
F. Tagliaferri
DIAS–Università degli Studi di Napoli, Federico II

Checked by:
A. Rößler / D. Hösel
TU-Chemnitz

DESIGN PREFERENCES

Examined plan types: Full/Fractional Factorial Design
Why: a screening plan is needed.

	Plan	Factors	Resolution	Test number (for 1 replication)	Replication number	Preliminary test number	Total test number	Tool Number (insert)	Selected
1.	2^{4-1}	1. Infeed $\mathbf{a_p}$ *(axial depth of cut)* 2. Feed per tooth $\mathbf{f_z}$ 3. Cutting speed $\mathbf{v_c}$ 4. Mode (laser on/off)	**IV** No main effects are aliased with any other main effect or 2-factor interactions, but some 2-factor interactions are aliased with other 2-factor interactions and main effects are aliased with 3-factor interactions.	8	1	0	8	3(insert) x 1(repl.) x 8(runs) / 2(edge)= 12	
2.	2^3	1. Infeed $\mathbf{a_p}$ *(axial depth of cut)* 2. Feed per tooth $\mathbf{f_z}$ 3. Cutting speed $\mathbf{v_c}$	**Full**	8	2	0	16	1(insert) x 2(repl.) x 8(runs) / 2(edge)= 8	
3.	2^3	1. Infeed $\mathbf{a_p}$ *(axial depth of cut)* 2. Feed per tooth $\mathbf{f_z}$ 3. Cutting speed $\mathbf{v_c}$	**Full**	8	1	0	8	3(insert) x 1(repl.) x 8(runs) / 2(edge)= 12	
4.	2^3	1. Infeed $\mathbf{a_p}$ *(axial depth of cut)* 2. Feed per tooth $\mathbf{f_z}$ 3. Cutting speed $\mathbf{v_c}$	**Full**	8	3	0	24	1(insert) x 3(repl.) x 8(runs) / 2(edge)= 12	**X**

5.	2^4	1. Infeed $\mathbf{a_p}$ *(axial depth of cut)* 2. Feed per tooth $\mathbf{f_z}$ 3. Cutting speed $\mathbf{v_c}$ 4. Mode (laser on/off)	**Full**	16	2	0	32	1(insert) x 2(repl.) x 16(runs) / 2(edge)= 16	
6.	2^{5-1}	1. Infeed $\mathbf{a_p}$ *(axial depth of cut)* 2. Feed per tooth $\mathbf{f_z}$ 3. Cutting speed $\mathbf{v_c}$ 4. Contact width $\mathbf{a_e}$ *(radial depth of cut)* 5. Mode (laser on/off)	**V** No main effects or 2-factor interactions are aliased with any other main effect or 2-factor interactions, but 2-factor interactions are aliased with 3-factor interactions and main effects are aliased with 4-factor interactions.	16	2	0	32	1(insert) x 2(repl.) x 16(runs) / 2(edge)= 16	

ANALYSIS AND PRESENTATION TECHNIQUES

ANOVA, Main effect plots, Interaction plots

TRIAL RUNS

Following trial runs were performed: NO TRIAL RUNS

CONTROL VARIABLE

Control Variable (Factor)	Normal level and range - Maximum acceptable range	Proposed settings, based on predicted effects	Predicted effects (for various responses)	Measurement precision and setting error How known?
Infeed $\mathbf{a_p}$ [mm] *(axial depth of cut)*	Max value: 11	[..]; [..] due to the high strength of the material and the small zone heated	-	
Feed per tooth $\mathbf{f_z}$ [mm/z]	0,075÷0,16	[..]; [..]	-	
Cutting speed $\mathbf{v_c}$ [m/min]		[..];[..]	-	

HELD CONSTANT FACTORS

Held-Constant Factor	Desired experimental level and allowable range	How to control (in experiment)	Anticipated effects	Measurement precision or range to which it can be measured How known?
Milling length **s** [mm]	85	It coincides with the workpiece length	-	
Number of teeth/cutting edge number **Z**	3 per tool; but 1 per tool for the tests	it cannot change	-	-
Tool diameter **D** [mm]	25	it cannot change	-	-
Angle in action **κ** [°]	90	it cannot change	-	

Cut-bend-angle **φ_s** [°]	=2*asin(ae/D) =2*asin(7mm/25mm)=32,52°	it cannot change	-	
Surface temperature **t** [°C]	500	by pyrometer	At elevated temperatures, the mechanical properties change, with yield strength decreasing and the material deformation behavior changing from brittle to ductile, thus reducing tool wear, improving surface finish and increasing material removal rates.	
Scanner speed **v_s** [mm/s]	50		-	
Contact width **a_e** [mm] *(radial depth of cut)*	7		-	
Mode (laser on/off)	Laser on	it cannot change	-	

NOISE FACTORS

Noise Factor	Anticipated effects	Strategy to reduce the noise factor impact on the results (e.g. randomization, blocking. etc.)	Measurement precision How known?

SECOND ORDER FACTOR INTERACTION

(predicted)

Control Factor	Feed per tooth $\mathbf{f_z}$ [mm]	Cutting speed $\mathbf{v_c}$ [m/min]	…	Mode (laser on/off)	
Infeed $\mathbf{a_p}$ [mm] *(axial depth of cut)*					
	Feed per tooth $\mathbf{f_z}$ [mm]				
		Cutting speed $\mathbf{v_c}$ [m/min]			
			…		
				Mode (laser on/off)	

ATTACHMENT II:

TECHNICAL REPORT - Tribological behavior of Micro-Structured materials

Technical Report

Topic:	Technische Universität Chemnitz
Organization:	Tribological Behavior of Partial Micro-Structured Bronze Materials
Testing objectives:	In literature, partial structuring is pointed out to be an efficient way to increase the load carrying capacity of a lubrication film. The major aim is to evaluate the effect of partial surface structuring on the characteristic friction stribeck curve. The important issue is to minimize friction and the transition velocity to hydrodynamic lubrication regime. The measurements are important for oil lubricated bearings with a high external load. The knowledge of the effects of microstructure geometry on the friction coefficient helps to select the microstructure geometry for a given load or load range (velocity, force).

ACTIVITIES

TASK	SUB-TASK	DETAILS	STATUS
Pre-design			
	Literature review	A brief review of international literature was performed	**Performed**
	Selection of response variables	Some potential response variables are selected (for details see attached pre-design guide sheets)	**Performed**
	Choice and definition of parameters	Some potential control factor are selected (for details see attached pre-design guide sheets)	**Performed**
	Definition of factor value ranges for testing (min-max)		In progress
Definition of design			
	choice of appropriate design of experiment	Some potential design of eperiment are selected (for details see attached pre-design guide sheets)	In progress

Prepared by:
F. Tagliaferri
DIAS–Università degli Studi di Napoli, Federico II

Rev. A
20/10/2011

TASK	SUB-TASK	DETAILS	STATUS
	use of specialized software to plan test's order	Not performed yet	In progress
Tests		Not performed yet	In progress
Laboratory analysis		Not performed yet	In progress
Statistical Analysis		Not performed yet	In progress
Technological interpretation of results		Not performed yet	In progress
Publication of results		Not performed yet	In progress

Pre-design guide sheets

GENERAL DATA

Responsible for testing:	Philipp Steinert
Organization:	Technische Universität Chemnitz
Topic:	Tribological Behavior of Partial Micro-Structured Bronze Materials
Testing objectives: (also in terms of response variables target values) should be unbiased, specific, measurable, and of practical consequence	In literature, partial structuring is pointed out to be an efficient way to increase the load carrying capacity of a lubrication film. The major aim is to evaluate the effect of partial surface structuring on the characteristic friction stribeck curve. The important issue is to minimize friction and the transition velocity to hydrodynamic lubrication regime. The measurements are important for oil lubricated bearings with a high external load. The knowledge of the effects of microstructure geometry on the friction coefficient helps to select the microstructure geometry for a given load or load range (velocity, force).

To remember:

	Steps of experimentation
1	**Recognition of and statement of the problem**
2	**Selection of the response variable(s)**
3	**Choice of factors and levels**
4	**Choice of experimental design**
5	Conduction of the experiment
6	Data analysis
7	Conclusions and recommendations

	Pre-design Guide Sheets	
1	Name, Organization, Title	
2	Objectives	
3	Relevant Background and Equipment	
4	Response Variables/Factors	Focus on supplem. sheets
5	Control Variables/Factors	
6	Factors to be "held constant"	
7	Nuisance factors	
8	Interactions	
9	Restrictions	
10	Responsibility for coordination	
11	Design preferences	
12	Analysis and presentation techniques	
13	Trial run?	

Prepared by:
F. Tagliaferri
DIAS–Università degli Studi di Napoli, Federico II

Checked by:
P. Steinert
TU-Chemnitz

Rev. Draft
18/10/2011

BACKGROUND

Relevant helpful results and information (on response and control variables) from previous experience, physical law, theoretical relationships, paper, specialist opinions, expert knowledge:	
n°**1**	**Source/reference:** **Helpful information for testing:**

Analytical relationships between the different process parameters:		**Legend:**
1. μ = Fr / Fn	**2. v = 2 * n * pi * Rr**	μ … friction coefficient Fr … friction force Fn … normal force v … (mean) sliding velocity n … rotational speed Rr … friction radius Ra … outer radius Ri … inner radius Mr … friction torque Pr … friction power p … contact pressure A … area
3. Rr = 2 / 3 * (Ra^3 – Ri^3) / (Ra^2 – Ri^2)	**4. Fr = Mr / Rr**	
5. Pr = v * Fr	**6. p = Fn / A**	
7. A = 2 * pi * (Ra^2 – Ri^2)		

EQUIPMENT

1.	Wazau Tribometer Test Rigs: TRM 500, TRM 5000 - Test Rig: Ring – Disk Setup - Oil Supply System - Personal Computer: Test Programs	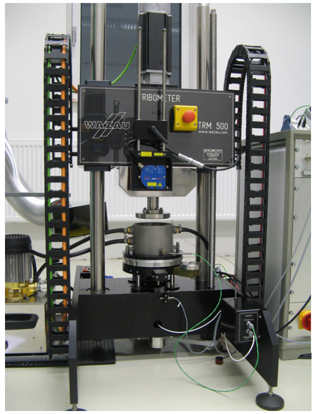
2.	ECM – Machine (Fraunhofer IWU), Micromachining by Anodic Dissolution of the Target Material	
3.	Samples - Steel Disc, Material 42CrMo4, grinded Diameter 100mm - Bronze Ring (structured), Material CuSn8, lathed	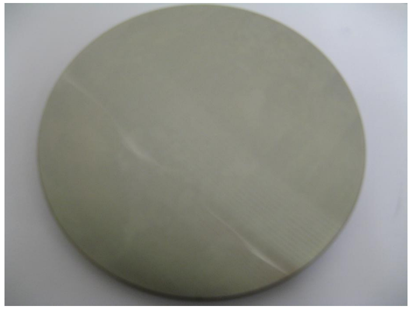 

RESPONSE VARIABLE

Response Variable	**Target** (relationship of response variable to objective)	**Normal operating level and range** (currently)	**Measurement precision, accuracy How known?**
μ [-] friction coefficient	minimize (to reduce wear and needed power)	0.05 – 1.00 or more (by formula 1 and 4, Mr is measured)	Range: 0 … 5 Nm Accuracy: +- 0.1% from calibration certificate

CONTROL FACTORS, HELD-COSTANT FACTORS, NOISE FACTORS

Factor	**Control**	**Held-Constant**	**Noise**	Why this choice? What is the alleged influence of the factor on the response variables?
Material properties		X		Tribological Behaviour is highly sensitive to Material Properties (Hardness, Thermodynamic Properties, Mechanical Properties etc.) of the Tribological System, always same test materials used
Normal force				Influence on the friction regime
Sliding velocity				Influence on the friction regime
Surface roughness		X		The sliding regime depends of roughness
Oil quality			X	Wear particles can intrude the contact area, this results in higher friction, chemical changes of the additives have an influence
Machining process surface		X		The kind of manufacturing the surface, influence on roughness
Machining process microstructure		X		not yet evaluated, possibilities: Jet-ECM, Laser Structuring

Structured area (%)	X			Literature & Simulation shows, that this influences the pressure generation in the lubrication gap
Structure Position	X			Literature & Simulation shows, that this influences the pressure generation in the lubrication gap
Calotte diameter		X		Literature & Simulation shows, that this influences the pressure generation in the lubrication gap
Calotte depth		X		Literature & Simulation shows, that this influences the pressure generation in the lubrication gap
Area density		X		Literature & Simulation shows, that this influences the pressure generation in the lubrication gap, higher is better
Temperature		X		This has strong influence on the oil viscosity
Lubrication condition		X		Dry, immersion, minimum lubrication
Intervention		X		Depends on the test sample geometry (is here the same in every test)
Time		X		Wear depends of time

CONSTRAINTS, LIMITATIONS AND RESTRICTIONS

1.	The normal force of the test rig is restricted to 5000 N
2.	The rotational speed is restricted to 3000 1/min
3.	The oil viscosity class was defined to 5W-30

MODE AND TIPS TO BE TAKEN INTO EVIDENCE

1.	

RESPONSIBILITY FOR COORDINATION

What	Who
ECM Calotte Machining	André Martin
Experimental investigation	Nancy Dietrich
Publication	Philipp Steinert

DESIGN PREFERENCES

Examined plan types: Full/Fractional Factorial Design
Why: a screening plan is needed.

	Plan	Factors	Resolution	Test number (for each replication)	Replication number	Preliminary test number	Total test number	Time Required	Selected
1.	2^3	1. Structured area (%) 2. Structure Position 3. Area density	**Full**	8	1	0	**8**		
2.	2^{4-1}	1. Structured area (%) 2. Structure Position 3. Area density 4. Calotte diameter	**IV** No main effects are aliased with any other main effect or 2-factor interactions, but <u>some 2-factor interactions are aliased with other 2-factor interactions</u> and main effects are aliased with 3-factor interactions.	8	1	0	**8**		

3.	2^4	1. Structured area (%) 2. Structure Position 3. Area density 4. Calotte diameter	**Full**	16	1	0	**16**		
4.	2^{5-1}	1. Structured area (%) 2. Structure Position 3. Area density 4. Calotte diameter 5. Calotte depth	**V** No main effects or 2-factor interactions are aliased with any other main effect or 2-factor interactions, but 2-factor interactions are aliased with 3-factor interactions and main effects are aliased with 4-factor interactions.	16	1	0	**16**		

Note for the user:

(from Douglas C. Montgomery & George C. Runger - 2003 - Applied Statistics And Probability For Engineers -John Wiley & Sons (3rd Ed))

The concept of interaction can be illustrated graphically in several ways. Figure 14-1 plots the data in Table 14-1 against the levels of A for both levels of B. Note that the B_{low} and B_{high} lines are approximately parallel, indicating that factors A and B do not interact significantly.
Figure 14-2 presents a similar plot for the data in Table 14-2.

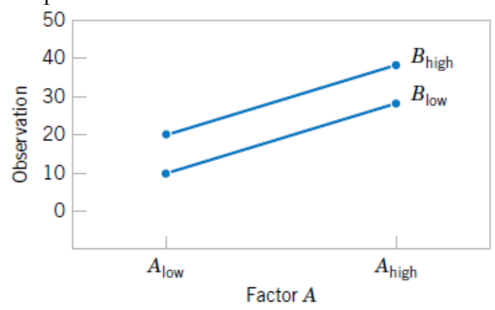

Figure 14-1 Factorial experiment, no interaction.

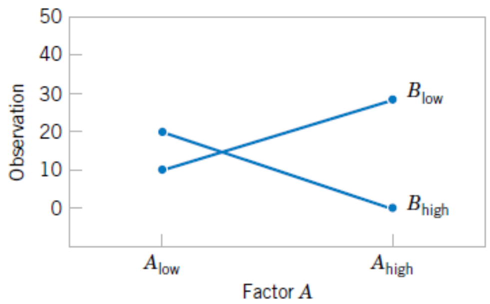

Figure 14-2 Factorial experiment, with interaction.

In this graph, the B_{low} and B_{high} lines are not parallel, indicating the interaction between factors A and B. Such graphical displays are called two-factor interaction plots. They are often useful in presenting the results of experiments, and many computer software programs used for analyzing data from designed experiments will construct these graphs automatically.

Figures 14-3 and 14-4 present another graphical illustration of the data from Tables 14-1 and 14-2. In Fig. 14-3 we have shown a three-dimensional surface plot of the data from Table 14-1. These data contain no interaction, and the surface plot is a plane lying above the A-B space. The slope of the plane in the A and B directions is proportional to the main effects of factors A and B, respectively. Figure 14-4 is a surface plot of the data from Table 14-2.

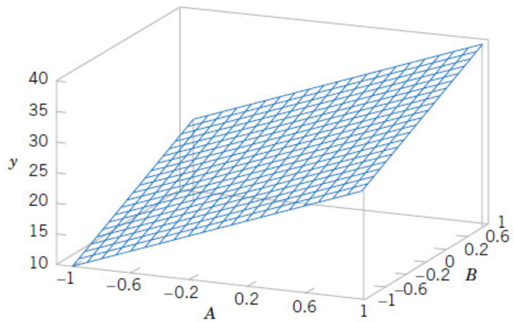

Figure 14-3 Three-dimensional surface plot of the data from Table 14-1, showing main effects of the two factors *A* and *B*.

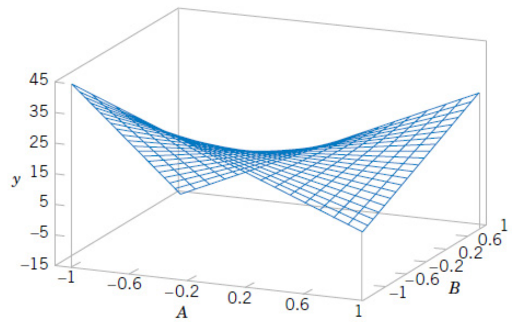

Figure 14-4 Three-dimensional surface plot of the data from Table 14-2 showing the effect of the *A* and *B* interaction.

Notice that the effect of the interaction in these data is to “twist” the plane, so that there is curvature in the response function. Factorial experiments are the only way to discover interactions between variables. An alternative to the factorial design that is (unfortunately) used in practice is to change the factors one at a time rather than to vary them simultaneously.

To illustrate this one-factorat-a-time procedure, suppose that an engineer is interested in finding the values of temperature and pressure that maximize yield in a chemical process.

Suppose that we fix temperature at 155_F (the current operating level) and perform five runs at different levels of time, say, 0.5, 1.0, 1.5, 2.0, and 2.5 hours. The results of this series of runs are shown in Fig. 14-5. This figure indicates that maximum yield is achieved at about 1.7 hours of reaction time. To optimize temperature, the engineer then fixes time at 1.7 hours (the apparent optimum) and performs five runs at different temperatures, say, 140, 150, 160, 170, and 180_F. The results of this set of runs are plotted in Fig. 14-6. Maximum yield occurs at about 155_F. Therefore, we would conclude that running the process at 155_F and 1.7 hours is the best set of operating conditions, resulting in yields of around 75%. Figure 14-7 displays the contour plot of actual process yield as a function of temperature and time with the one-factor-at-a-time experiments superimposed on the contours.

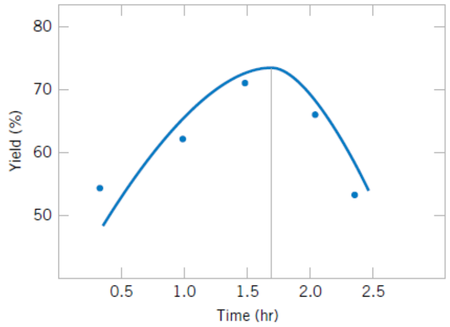

Figure 14-5 Yield versus reaction time with temperature constant at 155 °F.

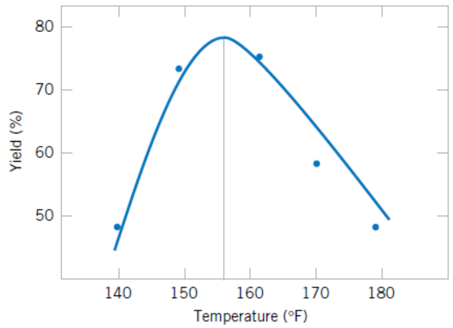

Figure 14-6 Yield versus temperature with reaction time constant at 1.7 hours.

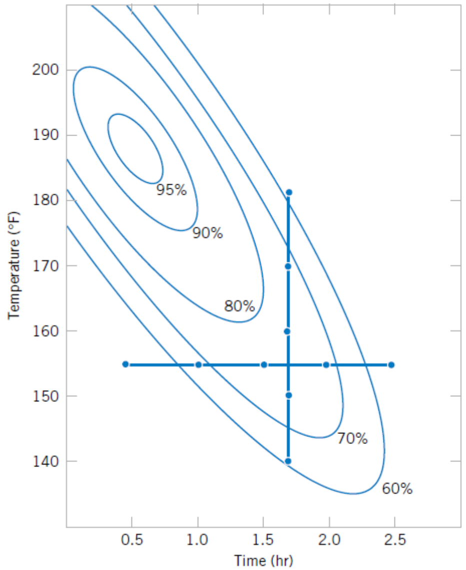

Figure 14-7 Optimization experiment using the one-factor-at-a-time method.

Clearly, this one-factor-at-a-time approach has failed dramatically here, as the true optimum is at least 20 yield points higher and occurs at much lower reaction times and higher temperatures. The failure to discover the importance of the shorter reaction times is particularly important because this could have significant impact on production volume or capacity, production planning, manufacturing cost, and total productivity. The one-factor-at-a-time approach has failed here because it cannot detect the interaction between temperature and time. Factorial experiments are the only way to detect interactions. Furthermore, the one-factor-at-a-time method is inefficient. It will require more experimentation than a factorial, and as we have just seen, there is no assurance that it will produce the correct results.

2^3 Design
This design is a 2^3 factorial design, and it has eight runs or treatment combinations. Geometrically, the design is a cube as shown in Fig. 14-18(a), with the eight
runs forming the corners of the cube. Figure 14-18(b) lists the eight runs in a table, with each row representing one of the runs are the - and + settings indicating the low and high levels for each of the three factors. This table is sometimes called the design matrix.

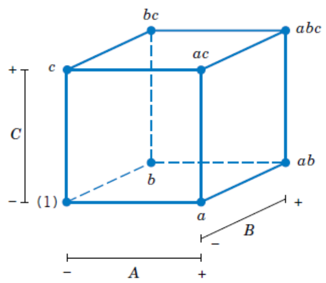

(a) Geometric view

Run	A	B	C
1	−	−	−
2	+	−	−
3	−	+	−
4	+	+	−
5	−	−	+
6	+	−	+
7	−	+	+
8	+	+	+

(b) The 2^3 design matrix

Figure 14-18 The 2^3 design.

This design allows three main effects to be estimated (A, B, and C) along with three two-factor interactions (AB, AC, and BC) and a three-factor interaction (ABC). The main effects can easily be estimated. The two-factor interaction effects may be computed easily. The ABC interaction is defined as the average difference between the AB interaction for the two different levels of C.

Design Resolution
The concept of design resolution is a useful way to catalog fractional factorial designs according to the alias patterns they produce. Designs of resolution III, IV, and V are particularly important. The definitions of these terms and an example of each follow.

1. Resolution III Designs. These are designs in which no main effects are aliased with any other main effect, but main effects are aliased with two-factor interactions and some two-factor interactions may be aliased with each other. The 2^{3-1} design with I = ABC is a resolution III design.
2. Resolution IV Designs. These are designs in which no main effect is aliased with any other main effect or two-factor interactions, but two-factor

interactions are aliased with each other. The 2^{4-1} design with I = ABCD used in Example 14-7 is a resolution IV design.
3. Resolution V Designs. These are designs in which no main effect or two-factor interaction is aliased with any other main effect or two-factor interaction, but two factor interactions are aliased with three-factor interactions. The 2^{5-1} design with I = ABCDE is a resolution V design.

Resolution III and IV designs are particularly useful in factor screening experiments. A resolution IV design provides good information about main effects and will provide some information about all two-factor interactions.

ANALYSIS AND PRESENTATION TECHNIQUES

ANOVA, Main effect plots, Interaction plots

TRIAL RUNS

Following trial runs were performed: NO TRIAL RUNS

CONTROL VARIABLE

Control Variable (Factor)	Normal level and range - Maximum acceptable range	Proposed settings, based on predicted effects	Predicted effects (for various responses)	Measurement precision and setting error How known?

HELD CONSTANT FACTORS

Held-Constant Factor	Desired experimental level and allowable range	How to control (in experiment)	Anticipated effects	Measurement precision or range to which it can be measured How known?

NOISE FACTORS

Noise Factor	Anticipated effects	Strategy to reduce the noise factor impact on the results (e.g. randomization, bloking. etc.)	Measurement precision How known?

SECOND ORDER FACTOR INTERACTION

(predicted)

Control Factor					

Prepared by:
F. Tagliaferri
DIAS–Università degli Studi di Napoli, Federico II

Checked by:
P. Steinert
TU-Chemnitz